SAPIENZA
Università di Roma
Facoltà di Farmacia e Medicina

Dottorato di Ricerca in
MORFOGENESI e INGEGNERIA TISSUTALE

XXX Ciclo
(A.A. 2016/2017)

HDAC inhibitors Modulate microRNA Content of Fibroadipogenic Progenitor-derived Exosomes to Promote Regeneration and Inhibit Fibrosis of Dystrophic Muscles

Dottorando
Martina Sandonà

Tutor
Dr. Pier Lorenzo Puri
Dr. Valentina Saccone
Prof. Marina Bouché

Coordinator
Prof. Sergio Adamo

Index

1. The thesis explained

This thesis aims to identify the extra-cellular mediators of the functional cross-talk between Fibro-Adipogenic Progenitors (FAPs) and Muscle Stem Cells (MuSCs) in Duchenne Muscular Dystrophy (DMD). For this purpose, we analyzed the role of extracellular vesicles (EVs) released by dystrophic FAPs to MuSCs, and performed a functional characterization of their microRNA content in response to HDAC inhibitors (HDACi) – a known epigenetic drug that modulate gene expression to promote regeneration and inhibit fibrosis in DMD, and is currently in clinical trial with DMD boys. We observed that FAPs-derived EVs exhibit standard features of exosomes, and their accumulation in muscle interstitial space of regenerating muscles suggests a role in promoting muscle regeneration.
Exosomes are nanovesicles involved in intracellular communication, which can transfer a cargo of genetic (mRNA, microRNA) or proteic information to recipient target cells. In order to decipher exosomal content transferred from dystrophic FAPs to MuSCs to support MuSCs myogenic activity, we analyzed microRNAs (miRs) cargo of FAPs derived exosomes. We found that exosomes from FAPs of mdx mice (the mouse model of DMD) that have been exposed to histone deacetylases inhibitor (HDACi) can replicate most of the beneficial effects of HDACi, including the increase in muscle regeneration and the inhibition of inflammation and fibrotic deposition. Transwell co-culture experiments show that exosomes from FAPs of mdx mice exposed to HDACi enhance muscle satellite cell (MuSCs) expansion and differentiation into myotubes. Of note, these exosomes showed enrichment in miRs involved into muscle regeneration, with the myomiR miR-206 being the most up-regulated. Functional evidence demonstrates that antagomiR-mediated targeting of miR-206 abrogated exosome ability to support MuSC expansion and formation of myotubes. We also performed a functional analysis of FAPs-derived exosomes by intramuscular injections of exosomes isolated from treated or

untreated dystrophic FAPs, previously transfected or not with antagomiR-206. We show that increased amounts of exosomal miR-206 are required for exosomes of HDACi-treated FAP-derived to promote compensatory regeneration and inhibit fibrosis in mdx muscles.
Our findings reported the first evidence of pharmacological manipulation of the miR content of cell type specific-derived exosomes to promote compensatory regeneration of dystrophic muscles. This evidence points to the potential for pharmacological modulation of FAP-derived exosome's content as tool for selective therapeutic interventions in muscular diseases.

2. Introduction

2.1 The skeletal muscle: a brief overview

Skeletal muscle is a plastic and dynamic tissue that forms the major bulk of our body mass. In general, muscle mass depends on a perfect balance between protein synthesis and degradation, that is influenced by different factors such as nutrition, hormone balance, physical exercise and disease. By its ability to convert chemical energy into mechanical energy, skeletal muscle contributes to the posture maintenance, breathing and movement production (Frontera and Ochala, 2015).
The histological and functional cellular units of mature skeletal muscle tissue are the muscle fibers that stretch along the entire length of any body muscle. Individual muscle fibers are packed tightly together into muscle fascicles with little intervening connective tissue called the *endomysium*. Fascicles are surrounded by the perimysium and many fascicles align themselves to give rise to the individual body muscles enveloped in the muscle fascia or the *epimysium* (Figure 1) (Yusuf and Brand-Saberi, 2012).

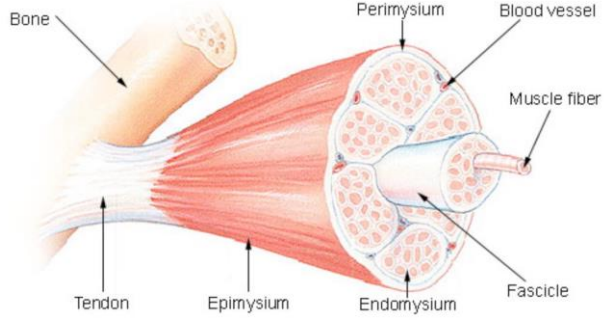

Figure 1 ***Schematic representation of skeletal muscle structure***

Each single muscle fiber is surrounded by sarcolemma that interacts with several proteins connected to the internal myofilament and allows the conservation of muscle structure. The two most abundant proteins in the skeletal muscle are actin and myosin, which compose approximately the 70-80% of the total protein content of the muscles and drive their contraction. However, there are many other proteins that contribute to the mechanical and physiological proprieties of muscles, such as troponins, titin, nebulin among others. Absence or dysfunction in one of these proteins leads to sarcolemma damage and to a specific disease (Frontera and Ochala, 2015). Evenly interspersed running embedded in the connective tissue are nerves and vessels that innervate and supply the muscle fibers. Thus, the functional properties of skeletal muscle depend on the maintenance of a complex framework of myofibers, motor neurons, blood vessels and extracellular connective tissue matrix (Yusuf and Brand-Saberi, 2012).
The heterogeneity and plasticity of skeletal muscle are due to the different types of myofibers - low-contracting/fatigue-resistant (oxidative) and fast- contracting/non-fatigue-resistant (glycolytic) and mixed fibers. Their proportion within a muscle determines their ability to allow low-intensity activity (e.g., posture), repeated submaximal contractions (e.g. locomotion) and fast and strong maximal contractions (jumping, kicking) (Chargé and Rudnicki, 2004; Schiaffino and Reggiani, 2011).

2.2 Phases of muscle regeneration

In physiological conditions, the skeletal muscle is a stable tissue characterized by a small turnover of multinucleated myofibers. However, this tissue is frequently exposed to injuries, such as direct trauma (e.g. intensive physical activities, lacerations) or resulting from indirect causes such as neurological dysfunction or consequence of genetic defect (e.g. muscular dystrophies leading to fiber degeneration post-contraction). In all these instances, skeletal muscle can activated rapid and extensive

processes of regeneration. If not repaired, chronic muscle injuries can result in loss of muscle tissue, defects in locomotion, and in the worse cases, premature death (Chargé and Rudnicki, 2004; Yusuf and Brand-Saberi, 2012).
The muscle regeneration process recapitulates many aspect of skeletal muscle development and it's characterized by five interrelated and time-dependent phases (Chargé and Rudnicki, 2004; Musarò, 2014). The initial event, named necrosis, is characterized by disruption of sarcolemma and increase of myofibers permeability (Figure 2). As a consequence of the disruption of the myofibers integrity, a rise of the serum levels of muscle proteins (such as creatine kinase) and muscle-specific microRNAs (miR-1, miR-133, and miR-206) occur, since they are normally restricted to muscle fibers. Increased serum levels of creatine kinase and muscle microRNAs can be found after mechanical stress as well as during muscle degenerative diseases such as muscular dystrophies (Zatz et al., 1991; Cacchiarelli et al., 2011). Calcium (Ca+)-dependent necrosis stimulates the second step of muscle regeneration: necrotic cell death recruits specific myeloid cell population within the injured area activating the inflammatory response (Tidball, 2005). Neutrophils are the first inflammatory cells to invade the injured muscle, a significant increase in their number it's observed in the first 6 hours after damage. After neutrophils infiltration they release high concentrations of free radicals and proteases, as well as pro-inflammatory cytokines that activate monocytes and macrophages, which remove tissue debris and activate stem cell populations (Figure 2). Two different populations of macrophages, M1 and M2, participate to functional regeneration. Briefly, M1 removes debris and produce pro-inflammatory cytokines supporting the appearance of M2. M2 produces anti-inflammatory cytokines and plays an important role in deactivating M1 and in the activation of satellite cells. Therefore, the inflammatory response must be finely regulated to obtain an efficient regenerative process; temporal and spatial

deregulation of these cells types results in a persistent rather than resolved inflammatory phase (Figure 2) (Musarò, 2014).
Muscle degeneration is typically followed by the activation of muscle repair, which follows a sequence of steps: regeneration, remodeling and maturation. Firstly, MuSCs (e.g. the muscle stem cells) break quiescence and proliferate throughout the injured area. After the expansion, a portion of them is committed to the myogenic lineage and differentiates to form new fibers or fuse into injured fibers. Newly formed myofibers are characterized by small caliber and centrally located myonuclei. Moreover, they are distinguished from other fibers for the expression of embryonic/developmental forms of myosin heavy chain (MyHC), which reflects de novo fiber formation. When fusion of myogenic cells is completed, the size of the myofibers increases and myonuclei move to the periphery of the fiber. The regeneration phase is followed by the remodeling stage, in which there is an activation of the extracellular matrix resulting in the stabilization of tissue that acts as scaffold for the new myofibers (Mutsaers et al., 1997). The last step is the completion of the muscle repair and it is completed when new myofibers become effectively innervated, leading to the acquisition of contractile ability. Finally, the repaired muscle tissue is morphologically and functionally equivalent to that uninjured (Figure 2) (Chargé and Rudnicki, 2004).

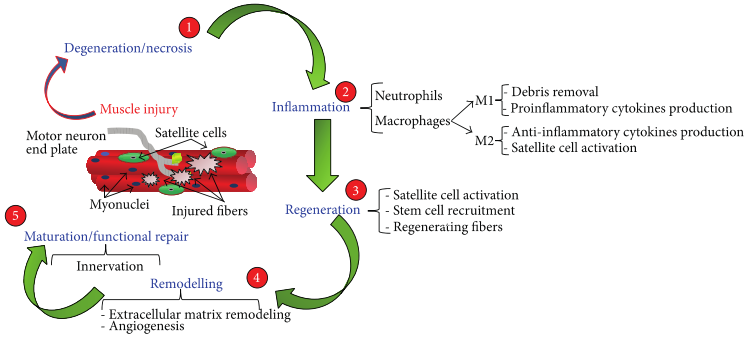

Figure 2 ***Schematic representation of muscle regeneration phases (Musarò, 2014).***

2.3 Cellular mediators of muscle regeneration

Muscle stem cells, known as satellite cells (MuSCs), represent the main player of muscle regeneration. Alexander Mauro discovered MuSCs in 1961; he described them as quiescent cells residing between the basal lamina and sarcolemma of myofibers, calling them "dormant myoblasts that failed to fuse with other myoblasts and are ready to recapitulate the embryonic development of the skeletal muscle fiber when the main multinucleate cell–is damaged" (Mauro, 1961). Indeed, several following studies examined in depth the ability of MuSCs to be activated upon injury; they proliferate, differentiate and fuse with damaged myofibers (Snow, 1977; Bischoff, 1986; Whalen et al., 1990).
MuSCs can adopt different divergent fates: upon stimulation most of them activate the differentiation program, while others withdraw from differentiation to maintain the satellite cells pool (Zammit et al., 2004).
Their myogenic lineage is determined by the expression of Pax3 and its paralogue Pax7 (members of the paired box transcription

factor family). Pax3 is essential for embryonic development (Bober et al., 1994), whereas Pax7 is necessary for the post-natal maintenance and self-renewal of MuSCs (Seale et al., 2000; Wang and Rudnicki, 2011). Pax7 is maintained in all MuSCs and proliferating myoblast, but is down regulated before differentiation (Olguin and Olwin, 2004). When MuSCs are activated they leave their niche and start to cycle and to co-express Pax7 and MyoD (basic helix loop helix transcription factor). Most of these Pax7-MyoD positive cells are destined to form new multinucleated myofibers; they down-regulated Pax7 and start to express myogenin (basic helix loop helix transcription factor) (Le Grand and Rudnicki, 2007). Others cells down-regulate MyoD and maintain Pax7, representing the self-renewing fraction that lead to a replenishment of MuSCs niche (Figure 3) (Zammit et al., 2004; Olguin and Olwin, 2004). The self-renewal process is essential for the homeostasis of skeletal muscle because is able to prevent, when recurrent muscle regeneration occurs, the depletion of MuSCs pool (Chargé and Rudnicki, 2004).

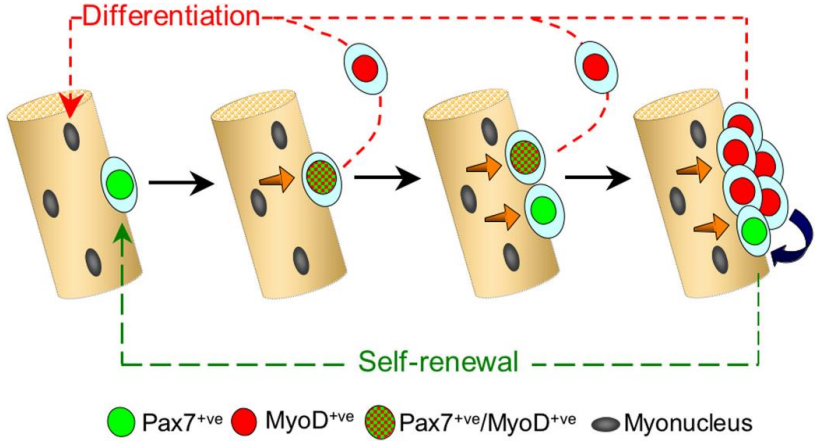

Figure 3 ***Model of MuSCs self-renewal (Zammit et al., 2004).***

The activation of MuSCs from quiescent state to a myogenic lineage is controlled by specific transcription factors, named Myogenic Regulatory Factors (MRFs) such as Myf5, MyoD, myogenin and MFR4 (Zammit and Beauchamp, 2001). Briefly, Myf5 and MyoD determine the myogenic lineage of MuSCs; Myf5 locus is active only in quiescent MuSCs, while MyoD starts to be expressed when they are activated (Rudnicki et al., 1993; Tajbakhsh et al., 1996; Beauchamp et al., 2000). Myogenin and MFR4 are involved in the expression of the terminal muscle phenotype (Figure 4) (Le Grand and Rudnicki, 2007).

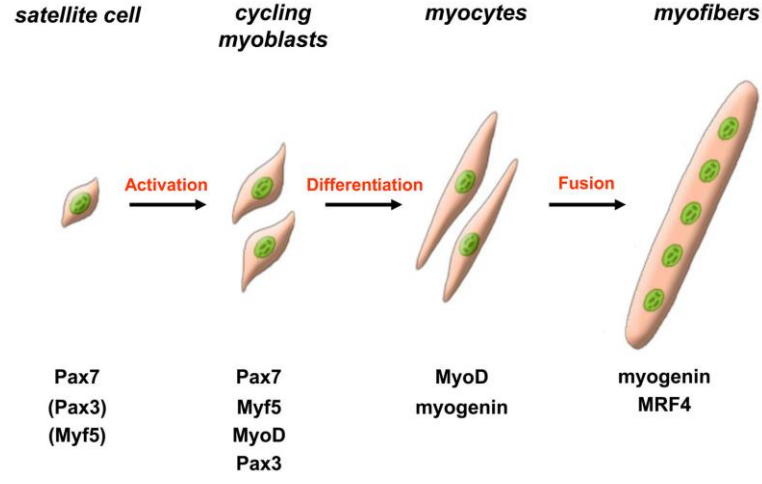

Figure 4 ***Schematic representation of activation, differentiation and fusion of MuSCs (Le Grand and Rudnicki, 2007).***

Although most of the regenerative response of skeletal muscle has been always attributed to MuSCs, recent discoveries have revealed the identity of additional mononuclear cells that compose the function niche of MuSCs. In particular, Fibro-Adipogenic Progenitors (FAPs) are cells with phenotypic and functional plasticity, as they can support MuSCs or adopt

fibrotic and adipogenic lineage (Joe et al., 2010; Uezumi et al., 2010).
FAPs are pluripotent cells resident in the interstitial position (that is, between fibers). They can be isolated by fluorescence activated cell sorting (FACS) as CD45-/ CD31- (lineage-negative lin-)/ Sca1+/ a7integrin- (Joe et al., 2010) or as lin-/ PDGFRa+/SM/C-2.6- cells (Uezumi et al., 2010). The environment which surrounds FAPs influences their phenotypical fate; in resting muscles functional interactions with intact myofibers prevents their conversion into fibro-adipocytes; however, upon muscle injury FAPs proliferate and release paracrine factors that contribute to promote MuSC-mediated muscle regeneration (Uezumi et al., 2010; Joe et al., 2010). By contrast, in degenerating muscles, these cells mediate fat deposition and fibrosis, disrupting the environment conducive for muscle regeneration (Uezumi et al., 2010; Uezumi et al., 2011). Therefore, FAPs seem to act as key sensors of muscle disruption, transmitting changes to muscle stem cells (Giordani and Puri, 2013).
Complete skeletal muscle repair is also dependent on two different subtypes of macrophages: pro-inflammatory (M1) and anti-inflammatory (M2) macrophages. Through a timely balanced pro- and anti-inflammatory waves, they regulate FAPs function and fate, which in turn determine the regenerative outcome, based on stimulation of MuSCs and transient or permanent deposition of extracellular matrix (ECM) (Muñoz-Cánoves and Serrano, 2015). Lemos *et al.* demonstrated the macrophages ability to influence FAPs fate and ECM accumulation in damaged muscle regulating the balance of pro-apoptotic (TNF) and pro-survival (TGFβ1) signals. For a successful regeneration process these two signals appear in two distinct times, while in chronic conditions of muscles damage, such as Muscular Dystrophies, they occur simultaneously, leading to an overlap of contradictory signaling (Lemos et al., 2015).

Other cell populations, termed side population (SP) cells, reside within muscle; these cells have myogenic potential and contribute to muscle regeneration. SP could be isolated from many tissues, such as bone marrow (bmSP) or muscle (mSP), but, *in vitro,* they are unable to undergo spontaneous myogenic differentiation. Upon SP intramuscular injection, they can give rise to both myocytes and putative MuSCs, thereby contributing to muscle regeneration (Asakura et al., 2002). Additional stem cell populations that have been isolated from adult skeletal muscle are: the muscle-derived stem cells (MDSCs) which are CD34+/Sca1+, located in the interstitium of skeletal muscle and contribute to the formation of new muscle fibers expressing MyoD and myogenin; PW1-Interstitial Cells (PICs) that express the cellular mediator PW1 and play an active role in regeneration, but do not seem to express an adipogenic phenotype, at variance with FAPs (Mitchell et al., 2010), and other non-muscle resident stem cells, like the cells derived from bone marrow (BMDCs) (Chargé and Rudnicki, 2004). Therefore, the complex mechanism of muscle regeneration is dependent upon a tightly interplay of different cell types in the muscle stem cell niche.

2.4 microRNA involved in muscle regeneration

MicroRNAs (miRs) are a class of evolutionally conserved non-coding RNAs of ~22 nucleotides, which regulate gene expression predominantly at the post-transcriptional level (Bartel, 2004). MiRs exert their function by binding 3'UTR of the mRNA target, leading to their translational inhibition and mRNA decay (Filipowicz et al., 2008).
MiRs are generated from intergenic or intragenic regions of the genome and they are transcribed mainly by RNA polymerase II as long primary transcripts, named pri-miRs. These pri-miRs are processed as ~70 bp pre-miR by the nuclear RNase III Drosha

and then exported to the cytoplasm by the Exportin-5. In the cytoplasm, mature miRs are produced by the pre-miR processing of the RNase III Dicer and, in this form, they can complete their activity (Kim et al., 2009).
MiRs are divided in two categories: miRs expressed in a tissue-specific manner, such as miR muscle specific (myomiRs) and others expressed in several tissues. Both categories are involved in tissue and organ development; in particular myomiRs are necessary for the control of myogenesis and for muscle homeostasis (Wang, 2013).
MiR-1, miR-133 and miR-206 belong to myomiRs category; miR-1 and miR-133 are expressed both in cardiac and skeletal muscles, while miR-206 is present only in skeletal muscle (McCarthy, 2011). The expression of these myomiRs is directly regulated by MRFs, in particular MyoD and MEF2 and SRF (serum growth factors) transcriptionally activate the expression of three pairs of muscle specific miRs: miR-1-1 and miR-133a-2 (clustered on mouse chromosome 2 and human chromosome 20) and miR-1-2 and miR-133a-1 (clustered on mouse and human chromosome 18) are regulated by SRF, MyoD and MEF2, while miR-206 and miR-133b (clustered on mouse chromosome 1 and human chromosome 6) are regulated specifically by MyoD (Figure 5) (Rao et al., 2006; Williams et al., 2009; Goljanek-Whysall et al., 2012). MiRs clustered together could be transcriptionally controlled in an independent manner; miR-133 increases myoblasts proliferation and decreases muscle differentiation, on the opposite miR-1 and miR-206 increases myoblasts differentiation and decreases their proliferation.

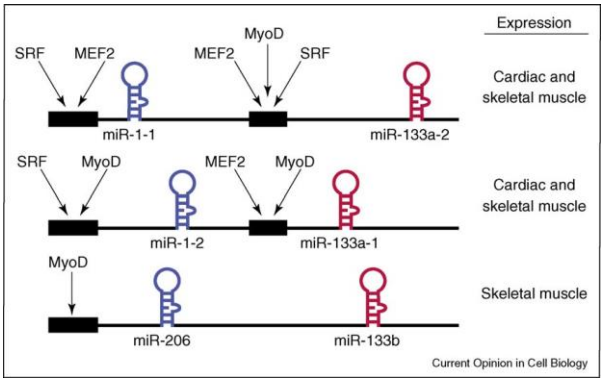

Figure 5 ***MRFs regulation of three bicistronic clusters of myomiRs (Williams et al., 2009).***

In particular, miR- 133 is able to induce myoblast proliferation by inhibiting two regulators of muscle differentiation: SRF and nPTB (polypirimidine tract binding protein) (Chen et al., 2006; Boutz et al., 2007), whereas miR-1 activates differentiation by targeting HDAC4, a transcriptional repressor of genes involved in muscles development. The inhibition of HDAC4 activates the expression of MEF2, which in turn promotes miR-1 expression. This negative feedback stimulates miR-1 ability to improve muscle differentiation (Chen et al., 2006). Moreover, miR-1 has as target a regulator of muscle growth and development, the insulin-like growth factor 1 (IGF-1) (Figure 6) (Elia et al., 2009).

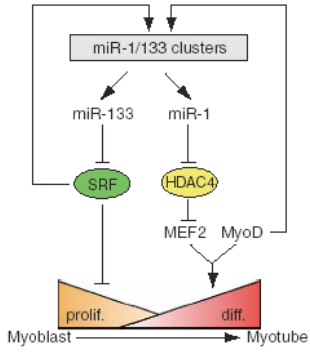

Figure 6 ***Model of miR-1 and miR-133 mediated regulation of skeletal muscle proliferation and differentiation (Chen et al., 2006).***

MiR-206 is one of the most characterized and studied miRs, which has several functions in muscle development and differentiation thanks to its very high number of targets (Ma et al., 2015). For example, miR-206 promotes differentiation through inhibition of a component of DNA polymerase, Pola1, and/or by targeting utrophin, follistatin-1 and also HDAC4 preventing their expression (Kim et al., 2006; Rosenberg et al., 2006; Winbanks et al., 2011). In addition, important miR-206 targets are Pax3 and Pax7; their timely down regulation by miR-206 is required for MuSCs and primary myoblast transition from proliferation to differentiation status (Chen et al., 2010; Hirai et al., 2010). A process of a feedback loop involves miR-206 in essential events of muscle differentiation: muscles injury up-regulates miR-206 expression that inhibits Pax3, Pax7 and c-Met promoting MuSCs differentiation; which in turn up-regulates MyoD and, therefore, miR-206 expression (Figure 7) (Chen et al., 2010; Dey et al., 2011).

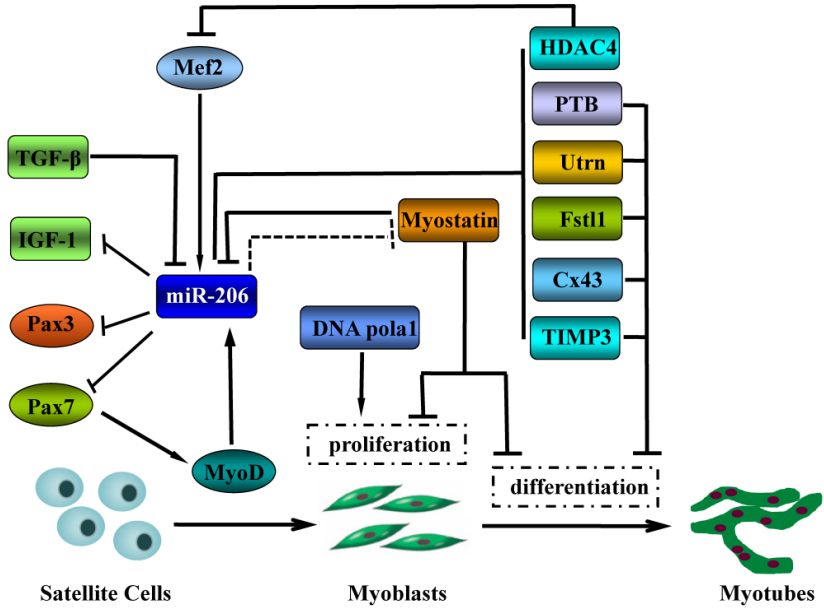

Figure 7 ***Molecular mechanism of miR-206 role in skeletal muscle development (Ma et al., 2015).***

Overall, muscle specific miRs family can be divided in three different classes based on their activity. The regenerative miRs, such as miR-206, miR-31, miR-34c, miR-335, miR-449 and miR-494; the degenerative miRs, between which miR-1, miR-29c and miR-135 and lastly, the inflammation-associated, such as miR-222 and miR-223 (Greco et al., 2009).
Other several miRs are involved in muscle differentiation. Some example are: miR-26a which targets the Polycomb group (PcG) Ezh2 methyltransferase, a negative regulator of muscle differentiation, thus favoring myogenesis (Wong and Tellam, 2008); miR-214, which also targets Ezh2 leading to a pro-myogenic switch (Juan et al., 2009), and miR-27b which targets Pax3, thereby inducing *in vivo* differentiation of muscle progenitor cells (Crist et al., 2009). These evidences underline the essential role of miRs in the regulation of different processes

that contribute to muscle regeneration suggesting the necessity to amplify studies on miRs targets and miRs involvement in muscle development.

2.5 Epigenetic regulation of skeletal myogenesis

Skeletal myogenesis is underpinned by specific epigenetic modifications. The combination of different post-translational modifications of histone tails (acetylation, methylation, phosphorylation and ubiquitination) modifies chromatin configuration, that influences the transcription of target genes of muscles development and regeneration (Fischle et al., 2003; Guasconi and Puri, 2009).
In undifferentiated myoblasts, HDACs (histone deacetylases) are recruited on the chromatin of muscle genes: Class I HDACs are associated with MyoD, while Class II HDACs are recruited on MEF2 (Mal et al., 2001; Puri et al., 2001; McKinsey et al., 2000). These interactions prevent the hyperacetylation on the regulatory elements of muscle genes, precluding the differentiation program. Other mediators of muscle gene repression are the methyltransferases. The chromatin repressive configuration following methylation of histone tails is driven by methyltransferase such as Suv39 h1 that determines methylation of H3 lysine 9 and component of Polycomb complex, Ezh2, that methylate H3 lysine 27 (Zhang et al., 2002; Caretti et al., 2004).
An additional and essential step to activate gene transcription is the chromatin remodeling within the nucleosome. Different chromatin remodeling complex have been characterized and the most studied is the SWI/SNF complex, which is able to induce permissive and repressive configurations for transcription. The SWI/SNF ability to promote or repress transcription is dependent upon the signaling activated in specific context; p38 (alpha and beta) activation promotes the recruitment of SWI/SNF complex on muscle promoters, whereas p38 gamma represses differentiation leading to the association of MyoD

with the histone methyltransferases KMT1A (Saccone and Puri, 2010).
The combination of different factors (Histone modification, Chromatin remodeling complex, miRs and MRFs) determines the epigenetic conditions towards the activation or repression of a specific subset of genes involved in skeletal myogenesis. Briefly, MRF-induced expression of miRs that target the repressive complexes, such as Polycomb and HDAC, supporting the de-repression of MRF-target genes and the activation of skeletal muscle differentiation processes (Saccone and Puri, 2010).

2.6 Duchenne Muscular Dystrophy (DMD): pathophysiology and therapies.

Muscular dystrophies include more than 30 different inherited diseases characterized by a rapid progression of muscle degeneration. The most severe form is the Duchenne muscular dystrophy (DMD), affecting approximately 1/3500 male birth. This disorder is caused by mutations in the dystrophin gene on the X chromosome that lead to the complete absence of the protein (Hoffman and Dressman, 2001). Different dystrophin mutations lead to DMD; including duplications of one or several exons, point mutations and in most cases deletions (Muntoni et al., 2003). If these mutations alter the reading frame of dystrophin (out of frame-mutation), the protein is not produced and the patient develops DMD. If the mutation is “in frame”, the dystrophin is smaller in size, but still functional, and the patients are diagnosed with the less sever Becker Muscular Dystrophy (BMD) (Manzur et al., 2008).
Dystrophin is a protein localized at the sarcoplasmic surface of the sarcolemma where it forms the dystrophin-glycoprotein complex (DGC) interacting with glycoproteins. DGC functions as a structural link between the extracellular matrix and cytoskeleton preserving cell integrity after mechanical stress

associated with muscle contraction. Dystrophin mutations lead to destruction of its binding with DGC leading to loss of structural stability and of proper mechanic-transduction signaling. Therefore, dystrophin-deficient myofibers show increased vulnerability to muscle contraction injury with consequent necrosis and progressive failure of regeneration. Necrosis and regeneration, that follow the degeneration state, tend to counterbalance the muscle loss (Consalvi et al., 2014).
The early stage of the disease is characterized by several cycles of degeneration and compensatory regeneration, but during the progression of the disease, regeneration potential of muscles declines until complete exhaustion at late stage, with replacement of muscles with fibrotic scars and adipose tissue (Hoffman and Dressman, 2001).
The mdx mouse is the mostly used animal model for DMD. It has a spontaneous mutation in exon 23 of the dystrophin gene that introduces a premature stop codon leading to the lack of the mature protein. The pathology of the mdx mouse is characterized by histologically well-defined stages with similarity to the human pathology. The onset of skeletal muscle necrosis is around 3 weeks of post-natal life, followed by an extensive period of degeneration and regeneration (3-4 months). However, contrary to the lethal human pathology, the mdx mouse somehow recovers from the progressive muscle wasting, and reaches the stabilization of the pathology, with the accumulation of connective and adipose tissues only in very late stage of the disease (De Luca, 2012).
Several strategies are under investigation for the management of DMD. They consist of three different approaches: gene, cellular, and pharmacological therapies.
The cell therapy postulates to directly provide, to the organism, the stem cells able to generate healthy muscle fibers producing functional dystrophin. In the last years different progenitors have been identified showing myogenic potential; these populations include mesoangioblasts (Sampaolesi et al., 2006), pericytes (Dellavalle et al., 2011), side population (SP) (Asakura

et al., 2002), muscle derived stem cells (MDSC) and PW1 interstitial cells (PICs) (Mitchell et al., 2010). The main obstacle that needs to be addressed is the immune response of the host body, in which dystrophin is absent (Strober, 2006).

The several gene therapies for DMD aim to re-introduce functional dystrophin or to repair the affected gene in dystrophic muscles. Because almost 70% of mutations responsible for DMD altered the reading frame, the result is a truncated non-functional dystrophin protein. Therapies for DMD are designed to skip an exon in the dystrophin mRNA to enable the synthesis of a shortened but partially functional form of dystrophin protein. This methodology named Exon Skipping, uses different antisense oligonucleotide in order to exclude one or more exons from the splicing machinery and cause their skipping during the splicing process, represents a potential therapeutic approach to correct for specific genetic mutations and restore production of dystrophin protein. The main limitation of this approach is that it cannot be used on large deletions.

An other gene strategy is Ataluren, which aims to modify the mRNA structure through the introduction of small molecules that induce the ribosomal subunits to substitute a mutation induced stop codon with a single amino acid. The re-insertion of gene strategy uses adeno-associated viruses that contain a functional dystrophin gene, in order to re-express it in affected muscle. The complication of the immune response in host body of the viral vector was exceed by the use of non-viral vectors such as plasmids, human artificial chromosomes (HACs) or transposons (Strober, 2006).

The pharmacological strategies, such as the myostatin and TGF-beta manipulation or transgenic expression of follistatin and activation of IGF-1, aim to promote the regenerative response, thus maintaining the integrity of the muscle during the progression of the disease. Other treatments aim to manipulate the inflammatory pathways; for example the inhibition of NF-kB, which controls many inflammatory genes, is a selective target for future therapeutic interventions. The directly action on

macrophages might also deregulate the inhibition mediated by NF-kB in the myogenic program of muscle precursors (Mozzetta et al., 2009).
A promising pharmacological therapy for DMD was found in the application of epigenetic drugs that manipulate skeletal myogenesis targeting the acetylation of histone or non-histone (e.g. MyoD, MEF2) proteins. These drugs are the inhibitor of histone deacetylases (HDACi). The rational beyond using of HDACi for DMD treatment resides on the evidence of a non-structural function of DGC. Dystrophin absence modulates DGC ability to regulate levels of nitric oxide (NO) that controls HDACs; in details, in dystrophic muscles there are low levels of NO that lead to a persisting binding of HDACII on myogenic genes and miR producing their transcriptional inhibition (Figure 8) (Colussi et al.,2008; Cacchiarelli et al., 2010).

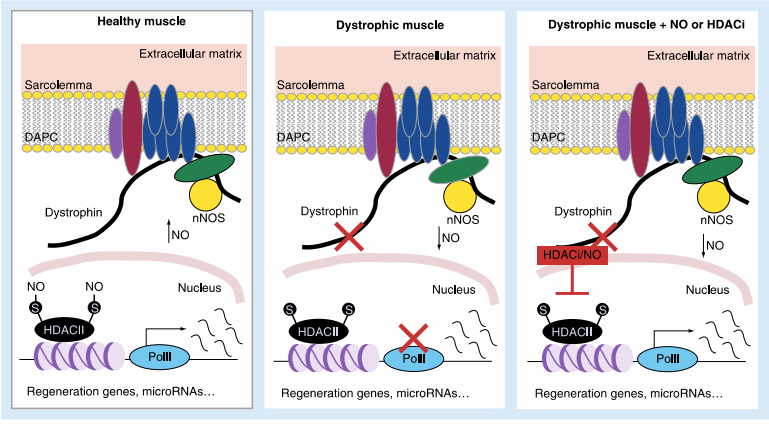

Figura 8 ***Schematic model of link between DMD and HDACs (Consalvi et al., 2014).***

Recent studies highlighted the stage specific ability of HDACi treatment (Trichostatin A –TSA- and Givinostat) to promote muscle regeneration and to decrease fibrosis and adipogenesis in

DMD muscle. The beneficial effect of these epigenetics drugs was observed only in early stages of DMD progression, in which there is still a regenerative permissive environment (Minetti et al., 2006; Consalvi et al., 2011; Consalvi et al., 2013; Mozzetta et al., 2013; Saccone et al., 2014). These studies determined the cellular target of HDACi treatment, the FAPs, and underlined a specific network, in which SWI/SNF complex and miR expression are involved, that drives these cells from a fibro-adipogenic to a myogenic phenotype. Moreover, it has been observed that HDACi treatment enhances FAPs role in muscle regeneration by improving their ability to support MuSCs differentiation (Mozzetta et al., 2013; Saccone et al., 2014). All together these evidences suggested that HDACi represent a promising strategy to treat dystrophic muscles.
Preclinical studies of HDACi treatment on mdx mice (Minetti et al., 2006; Consalvi et al., 2013) lead to the first clinical trial of an epigenetic drug on DMD boys (8-10 years old). The HDACi Givinostat completed the phase II of clinical trial and, given absence on side effects and presence of positive effects on histological and functional parameters, is currently on-going (Bettica et al., 2016). A phase III multicenter trial, with over 100 patients is planned to start in 2018.

2.7 Extracellular vesicles (EVs): focus on exosomes.

Cells exchange information with other cells through different mechanisms: secretion of soluble factors, direct interaction and in addition through the release of membrane derived vesicles (EL Andaloussi et al., 2013). First evidence of vesicles were demonstrated in the 1983-1984, when two different groups observed multivesicular bodies ability to release vesicles in the extracellular space (Pan and Johnstone, 1983; Harding et al., 1984). Initially, extracellular vesicles (EVs) were regarded as membrane debris without any biological activity. Only in the 1996, Raposo showed a biological function of EVs; in particular he demonstrated EVs involvement in the stimulation of adaptive

immune response (Raposo et al., 1996). To follow, EVs activity was affirmed in numerous studies, increasing the biological interest on EVs (Théry et al., 2009; Chaput and Théry, 2011; Lee et al., 2012; Ratajczak et al., 2012).
EVs are classified based on their size, density, morphology, lipid component, proteins, cellular origin and biological functions (Théry et al., 2009). The three main categories of EVs are: apoptotic bodies, microvesicles and exosomes (Table 1).

Extracellular vehicles	Size	Biogenesis	Characteristics	Content	Role
Apoptotic bodies	50–5000 nm	Broad plasma membrane blobbing and breach of cell fragments	Heterogeneous group of vesicles; contains surface markers for the recognition by phagocytic cells markers: Annexin-V	Fragmented nuclei as well as cytoplasmic organelles, histone, DNA fragments	Activated as response to a cellular stress or injury
Microvesicles	50–1000 nm	Bud directly from the plasma membrane through unique cellular mechanisms	No characteristic markers; lack of transferrin receptors; secreted during normal cellular processes	Cellular proteins, lipids and RNA, including miRNAs	Intercellular communication; transfer of proteins and genetic material
Exosomes	30–150 nm	Originate from the endosomal network named multivesicular bodies (MVBs) and released upon MVB fusion with the plasma membrane	More homogenous in size than other vesicles; highly enriched in transferrin receptors; secreted during normal cellular processes; markers: CD9, CD63, Alix, flotillin-1 and Tsg101	Cellular proteins, lipids and RNA, including miRNAs	Intercellular communication; transfer of proteins and genetic material

Table 1 ***Characteristic of three different categories of EVs (Braicu et al., 2015).***

Exosomes are the smaller EVs, with a range of size between 30 and 150 nm, their characteristic buoyant density is approximately of 1.10 to 1.21 g/ml in sucrose and aside their lipids such as ceramide, cholesterol and sphingolipids, their composition consists of proteins like Rab GTPases, heat shock protein 70, annexins, TSG101, Alix and tetraspanins (CD63, CD9, CD81 and CD82) (Théry et al., 2002). The "classic" pathway of exosomes biogenesis involved the formation of intraluminal vesicles within the multivesicular body (MVB). The maturation of MVBs in late MVBs leads to the release of exosomes in to the extracellular space after their fusion with the plasma membrane. However, late MVBs can lead also to the

degradation of their cargo by the fusion with lysosomes (Figure 9) (Kowal et al., 2014).
Exosomes biogenesis is still a constantly evolving topic. So far, two different mechanisms are accepted for the ILVs formation: Endosomal Sorting Complex Required for Transport machinery (ESCRT) dependent and neutral sphingomyelinase dependent mechanisms. ESCRT consists of 4 complexes associated with proteins such as Alix and TSG101 (Théry et al., 2001). These 4 complexes work together to sort cargo into exosomes and to designate MVBs for degradation or release of exosomes (Figure 9) (Katzmann et al., 2001; Michelet et al., 2010; Baietti et al., 2012; Henne et al., 2013; Colombo et al., 2013). While, neutral sphingomyelinase converts sphingomyelin to ceramide, which allows the release of exosomes in the extracellular space (Trajkovic et al., 2008; Marsh and van Meer, 2008).

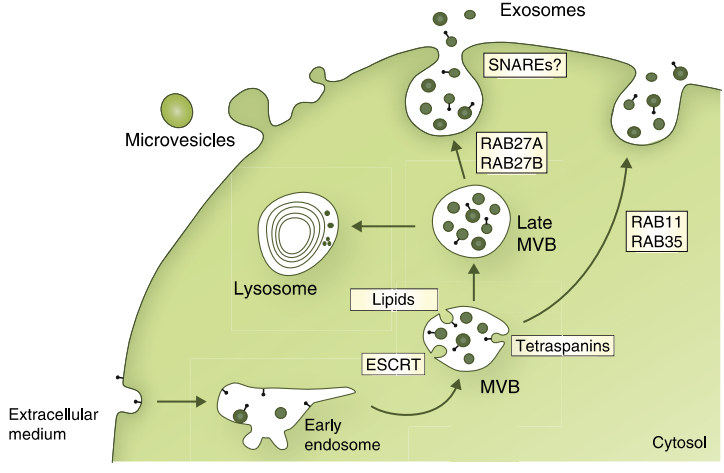

Figure 9 ***Intracellular machineries of exosomes biogenesis and secretion (Kowal et al., 2014).***

Next to the "classical" pathway of exosomes biogenesis, there is a more immediate mechanism of exosomes formation observed

in T-cells and erythroleukemia cells; the direct release of exosomes from the plasma membrane (Booth et al., 2006; Fang et al., 2007; Lenassi et al., 2010).
Exosomes are released in the extracellular space by most cells and are able to mediate intercellular communication via the transfer of genetic information, including the transfer of both coding and non-coding RNAs, to recipient cells (Figure 10) (Braicu et al., 2015).

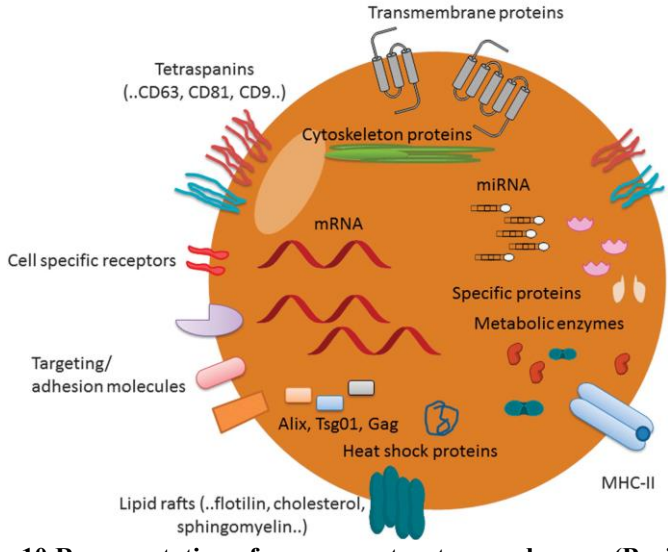

Figure 10 Representation of exosomes structure and cargo (Braicu et al., 2015).

Their content represents an instrument that cells used to modulated different mechanisms in several tissues and organs. The beneficial effects of exosomes include stem cells plasticity, alteration of immune response and effect on nervous system through the release of trophic factors (Lee et al., 2012). Interestingly, transferring their cargo, exosomes are able to contribute also to organ development, tissue repair and regeneration (Borges et al., 2013; Nakamura et al., 2015; Basu

and Ludlow, 2016; Fry et al., 2017). On the other hand, several studies demonstrated detrimental effects of exosomes showing their role in several pathologies, such as tumors, Alzheimer and Parkinson diseases (Théry et al., 2002; Lee et al., 2012; Raposo and Stoorvogel, 2013).

Therefore, the exchange of exosomes cargo represents a promising mechanism of genetic information transport and stem cell plasticity regulation via epigenetic reprogramming, which encourage the possibility of exploiting exosomes for therapeutic purposes (Valadi et al., 2007; Lee et al., 2012).

Multiple cell types have been described to release exosomes in extracellular medium, including mesenchymal cells, adipocytes, fibroblasts, immune cells and myoblasts. In particular, it is well known that muscles secrete exosomes (Guescini et al., 2010; Romancino et al., 2013; Forterre et al., 2014). Myoblasts and myotubes use exosome clustered miR as "endocrine signals" to control important signaling pathways (e.g. Wnt signaling pathway) for muscle homeostasis and regeneration. Exosome miRs secreted by myotubes are functionally able to silence Sirt1 in myoblasts, controlling their commitment to differentiation (Forterre et al., 2014).

Exosomes also mediate communication between distally located cells and tissue. For instance tumor cells promote muscle loss in cancer cachexia via exosome-assembled miR-21, which signals through the Toll-like 7 receptor (TLR7) on myoblasts to promote cell death (He et al., 2014). Of note exosomes appear to be naturally equipped to mediate tissue regeneration and their cargo may constitute a rapid response, protected by the oxidative environment, to initiate tissue repair (Saccone et al., 2014).

Exosomes are found *in vivo* in many biological fluids including blood, saliva, urine, and breast milk (Vlassov et al., 2012). Therefore, circulating miRs packed into exosomes could be useful biomarkers to determine various interactions between cells and also to monitor the development and progression of diseases.

3. Aims

This work focus on the identification of the soluble factors involved in the interaction between two essential players in the muscle stem cell niche that regulate the regenerative ability of skeletal muscles in physiological and pathological conditions: satellite cells (MuSCs) and Fibro-Adipogenic Progenitors (FAPs).

FAPs are muscle interstitial cells that in a regenerative environement, stimulate MuSCs proliferation and differentiation contributing to muscle regeneration. Our recent studies highlighted the role of FAPs in muscle regeneration of dystrophic muscle. At early stage of Duchenne Muscular Dystrophy (DMD), FAPs support myogenic activity of MuSCs while contribute to muscle degeneration at late stage of the diesease. Moreover, we identified FAPs as cellular target of treatment with inhibitors of histone deacetylases (HDACi); the first epigenetic drug used to counteract muscle degeneration in DMD. Briefly, we observed that HDACi treatment increases muscle regeneration and reduces muscle fibrosis and inflammation, furthermore we showed that HDACi improves FAPs ability to support MuSCs mediated regeneration. All these evidences have made the study of intracellular communication between FAPs and MuSCs necessary. Therefore, the goal of this project is to discover the molecular mediators of this cross-talk and to identify genetic information exchanged after HDACi treatment, useful for activation of muscle regeneration. As possible mediators we focused our attention on extracellular vesicles (EVs), which are discovered as essential molecules involved in intracellular communication, thanks to their ability to exchange genetic materials from a cell to another, both nearby and at long distance.

In this work we have focused on the following specific aims:

-Aim 1: Identification and characterization of mediators involved in the communication between young dystrophic FAPs and MuSCs. We performed co-culture experiments using a

transwell insert, which allows the indirect interactions between cells only through soluble factors. To identify the involvement of extracellular vesicles (EVs), we stained FAPs with PKH67 or transfected with CD63-GFP in order to have green EVs released by FAPs and to verify their ability to be uptaken by MuSCs. Assessed their role, we characterized size and markers of these FAPs-released EVs. By Dynamic Light Scattering (DLS), Scanning Electron Microscopy (SEM) and western blot analysis, we elucidated the nature of these EVs, identifying them as exosomes.

-Aim 2: Characterization of FAPs derived exosomes cargo. Starting from the knowledge of FAPs ability to support MuSCs differentiation and HDACi treatment to improve this beneficial effect through a miR mediated network, we analyzed miRs content of treated FAPs exosomes, performing a microRNA array, and deciphered their role in FAPs-MuSCs communication.

-Aim 3: We examined the effect of HDACi-treated FAPs derived exosomes in order to study their ability to promote muscle regeneration and inhibit muscle degeneration in mdx mice. In other words, we investigated FAPs derived exosomes power to mediate beneficial effect of HDACi treatment *in vivo*, performing intramuscular injection of exosomes in mdx mice and analyzing different histological parameters.

4. Results

4.1 FAPs promote MuSCs differentiation into multinucleated myotubes by Extracellular Vesicles.

Recent studies have revealed the crucial role of fibro-adipogenic progenitors (FAPs) in muscle regeneration. Upon muscle damage, the inflammatory infiltrate activates FAPs, which in turn stimulate Muscle Stem Cells (MuSCs) activation, suggesting the key role of FAPs in converting inflammatory cues into the signals that regulate MuSCs activity (Heredia et al., 2013; Lemos et al., 2015). In dystrophic muscles, it was observed that FAPs, normally quiescent, are activated and turn into fibro-adipocytes, which mediate fibrotic and fat deposition (Uezumi et al., 2011). On the other hand, in a permissive regenerative environment, typical of early stages of the Duchenne Muscular Dystrophy (DMD), dystrophic FAPs are able to promote MuSCs differentiation and contribute to muscle regeneration. The FAPs ability to support MuSCs mediated regeneration in dystrophic muscle is enhanced by the treatment with the inhibitors of histone deacetylases (HDACi) (Mozzetta et al., 2013). These evidences imply reciprocal communication between muscular cell populations in the regulation of muscle homeostasis and regeneration, through the exchange of soluble mediators, which are largely unknown.
To determine the identity of the soluble mediators of FAP's support to MuSCs in DMD muscles, we performed transwell co-cultures between FAPs isolated from 1.5-month-old mdx mice (time point that represents early stage of DMD progression) and MuSCs isolated from age-matched mdx mice. Cells are separated by a membrane of 1 mm pore size that prevents direct cell contact, yet allows reciprocal transfer of soluble mediators of functional interactions between co-cultured cells. To test the role of Extracellular Vesicles (EVs) in this cross-talk, we analyzed MuSCs differentiation in multinucleated myotubes after co-culture with FAPs treated or not with an inhibitor of

EVs biogenesis (GW4869). This drug is an inhibitor of neutral sphingomyelinase 2, an enzyme involved in converting sphingomyelin to ceramide, leading to a block of EVs, and in particular exosomes, secretion in the extracellular space (Kosaka et al., 2010). Myosin Heavy Chain (MyHC) staining assessed the MuSCs differentiation potential. By this experiment, we observed that FAPs (+FAPs DMSO) enhanced the ability of co-cultured MuSCs to differentiate into multinucleated myotubes, as compared to MuSCs cultured alone (-), and that exposure to GW4869 abrogated this ability (+FAPs GW) (Figure 11A and B). This evidence indicates that EVs are essential contributors of FAP-mediated support to MuSCs activity, and implies that FAP-delivered EVs are transferred to MuSCs, influencing MuSC biological properties. To directly test this possibility, we performed a transwell co-culture in the same conditions described above, but we previously incubated FAPs, treated or not with GW4869, with the lipidic dye (PKH-67). The staining with PKH-67 in FAPs allows the incorporation of the lipidic dye in EVs derived form FAPs, making possible the tracing of their passage to acceptor cells. PKH-67 staining was invariably detected in FAPs exposed to the dye, and in MuSCs co-cultured with PKH67-labelled FAPs (PKH-67 DMSO); however, exposure to GW4869 almost completely prevented (more than 80%) the detection of the signal in MuSCs co-cultured with FAPs (PKH-67 GW), indicating that FAP-derived EVs are uptaken by MuSCs (Figure 11C and D). To further investigate, and confirm, FAPs ability to release EVs to MuSCs, we repeated co-culture experiment between these two cell populations, but this time tracing EVs through GFP-CD63, an integral membrane protein enriched in EVs fused with GFP, transfection. FAPs was transfected with GFP-labeled CD63 (CD63-GFP) prior to transwell co-culture with the “acceptor” cells, MuSCs (Figure 11E). In this system, detection of GFP into MuSCs revealed the transfer of CD63-labelled EVs from FAPs to MuSCs. We show that GFP signal was detected in FAPs after transfection with GFP-CD63, but also in MuSCs co-cultured

with FAPs previously transfected with GFP-CD63, whereas no GFP signal was detected in MuSCs co-cultured with FAPs previously transfected with a control plasmid (Mock), confirming FAPs ability to release EVs that can be uptaken by MuSCs (Figure 11E).

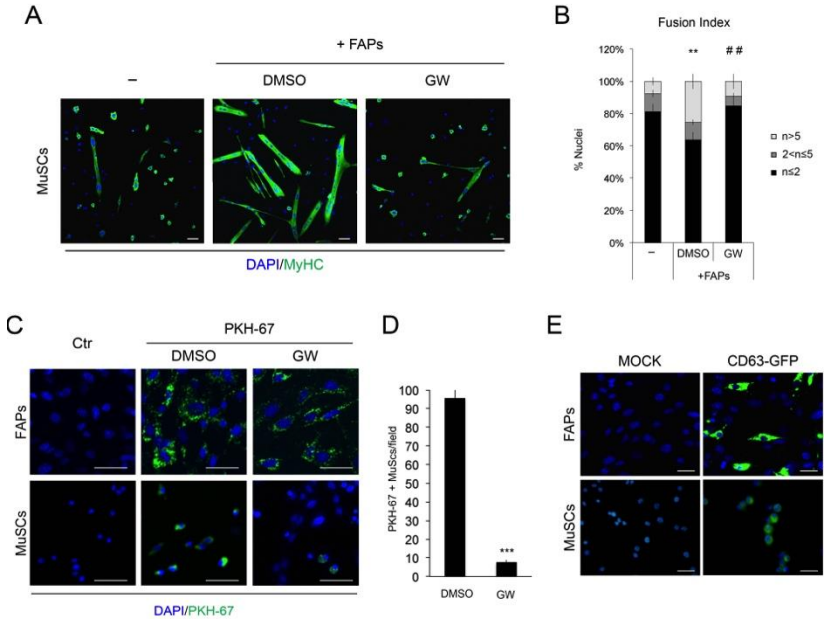

Figure 11 ***Extracellular vesicles from FAPs mediate the functional cross-talk with MuSCs.***
A) Representative images showing the myogenic differentiation of MuSCs assessed by immunostaining for MyHC (green). Nuclei were counterstained with DAPI (blue). MuSCs were cultured alone (-) or in transwell co-culture with FAPs treated with DMSO or GW4869 (GW). Scale bar = 50 μm. **B**) Graph showing the fusion index of MuSCs in the conditions described in A. n<2 indicates the percentage of nuclei that were $MyHC^-$ or $MyHC^+$ in mononucleated myotubes. 2 <n< 5 indicates the % of nuclei that were $MyHC^+$ inside myotubes containing between 2 and 5 nuclei. n>5 indicates the % of nuclei that were $MyHC^+$ inside myotubes containing more than 5 nuclei. Star (*) indicates statistical analysis by t-test relative to MuSCs

cultured alone (-). ** $p < 0.01$. Hash (#) indicates statistical analysis by t-test relative to MuSCs in co-cultured with FAPs not treated (DMSO). ## $p<0.01$. **C**) Representative images of PKH-67 (green) and DAPI (blue) staining in a transwell co-culture experiment showing EVs/exosomes transfer from FAPs to MuSCs. FAPs have been stained with PKH-67 or not (Ctr) and treated with DMSO or GW4869 to inhibit EVs biogenesis. Scale bar = 25 μm. **D**) Graph showing the percentage of PKH-67 positive MuSCs after the co-culture with FAPs treated with DMSO or GW4869 (GW) as described in C. Star (*) indicates statistical analysis by t-test. *** $p < 0.001$. **E**) Representative images of GFP detection (green) in MuSCs and FAPs co-cultured in transwell. Nuclei were counterstained with DAPI (blue). FAPs were previously transfected with mock (control GFP-plasmid) or GFP-CD63 plasmid. Scale bar = 25 μm.

4.2 Extracellular vesicles released by FAPs display typical features of exosomes.

EVs can be divided in three different categories with different characteristics, such as origin, size, density and protein markers. In order to define to which categories EVs released by FAPs belong, we performed three different experiments of characterization. In details we analyzed the size of EVs with Dynamic Light Scattering (DLS) and Scanning Electron Microscopy (SEM) while, through Western Blot (WB) analysis we identified EVs markers. For DLS analysis, we isolated EVs from serum-free media of dystrophic FAPs using two different procedures: precipitating agents (Total Exosome Isolation Reagents, Invitrogen -TEIR), or the standard differential ultracentrifugations (UC) (Théry et al., 2006). DLS showed, for EVs isolated with both protocol, an average of hydrodynamic diameter of about 150 nm that is consistent with the size of exosomes (Figure 12A) (Raposo and Stoorvogel, 2013). Moreover, this analysis determined that the two protocols are comparable. For this reason we decided to proceed using only TEIR to isolate exosomes. DLS results were also complemented with SEM analysis that confirmed that FAP-derived vesicles

(Exo-FAPs) ranged from 100-150 nm in size (Figure 12B). Moreover, a western blot analysis of the proteins content showed that presumptive exosome markers were abundantly expressed in vesicles (Exo) isolated from FAP's supernatant, including Alix, Hsp70, and to a less extent Flotillin1 and CD63. By contrast, Calnexin, a ubiquitously expressed ER protein, was exclusively found in FAP's whole cell fractions (WCL) (Figure 12C). Collectively, these data demonstrate that functionally active FAPs-derived EVs display typical features of mammalian exosomes (Lötvall et al., 2014) and will therefore be indicated therein as exosomes.

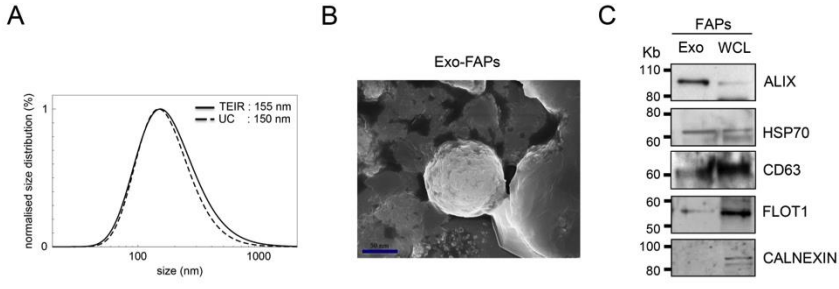

Figure 12 ***FAPs release Extracellular vesicles with physical features of Exosomes.***
A) Dynamic light scattering (DLS) analysis showing the size of FAPs-derived extracellular vesicles (EVs) isolated by total extracellular vesicles isolation reagent (TEIR) or ultracentrifugation (UC). **B)** Scanning electron microscopy of an exosome purified from FAPs cell culture serum free media using TEIR. **C)** Exosomes characterization by Western blot analysis for Alix, Hsp70, CD63, Flotilin1 (Flot1) and Calnexin antibodies in exosomes purified from FAPs cell culture serum free media (Exo) and in the cell lysate (WCL).

4.3 Muscle interstitial exosomes increased upon physiological and pathological regeneration.

Muscle regeneration is a typical process that occurs when muscle is damaged. One of the most reproducible methods to induce muscle regeneration is based on cardiotoxin (CTX) injection, a peptide that is isolated from snake venoms and acts as protein kinase C-specific inhibitor. CTX produces a local myonecrosis and stimulates muscle regeneration. 2-4 days post-injury, this process is characterized by MuSCs invasion and pick of regeneration that culminate in a total rescue of muscle damage 15-20 days post injury (Musarò, 2014).
Dystrophic muscles are characterized by an impairment of muscle homeostasis. The lack of dystrophin leads to myofibers damage, resulting in an activation of muscle regeneration. At early stage of the disease muscle is characterized by several cycles of degeneration and regeneration, which lead to an exhaustion of muscle regeneration potential during the progression of the pathology. Then, at late stages of DMD muscles are unable to regenerate and fibrotic scars and fat infiltration replace them. Recent studies demonstrate that treatment with Inhibitors of Histone Deacetylases (HDACi) improves muscle regeneration in a permissive environment (1.5-months old mdx mice), while they are not able to regress muscle degeneration in late stages of disease progression (1 years old mdx mice) (Minetti et al., 2006; Consalvi et al., 2013; Mozzetta et al., 2013; Saccone et al., 2014).
To investigate whether FAP-derived exosomes could be detected during muscle regeneration in physiological (CTX) versus pathological conditions (mdx), we performed *in situ* immunofluorescence for CD63 on muscle sections from young WT unperturbed (CTR) or regenerating muscles (3 days post injury- cardiotoxin injection-CTX), and from the mouse model of DMD – the mdx mice – either 1.5-month young or 1 year old, exposed or not to the HDACi Trichostatin A (TSA).

This analysis revealed sporadic CD63 signal (Red) in WT unperturbed and old mdx muscles, while a dramatic increase in CD63 signal was observed in regenerating WT and mdx young muscles. Interestingly, in all experimental conditions the vast majority of CD63 signal was invariably detected in the interstitium between regenerating, eMyHC-positive fibers (Cyan), and largely overlapped with interstitial Sca-1 signal (Green), which identifies putative FAP cells. Notably, muscle of mdx young mice exposed to TSA, which are characterized by an active regeneration, showed a significative increase of CD63 positive interstitial signal, as compared to young mdx CTR muscles, with similar levels to those observed in WT CTX muscles. By contrast, TSA treatment could not increase the CD63 signal in the interstitium of 1 year old muscles (Figure 13A and B). The overlap of interstitial CD63 and Sca1 signals and their close proximity to eMyHC-positive regenerating myofibers, together with the differential response of young or old mdx muscles to HDACi, suggest that FAP-derived exosomes could be implicated in HDACi-mediated activation of MuSCs to regenerate dystrophic muscles.

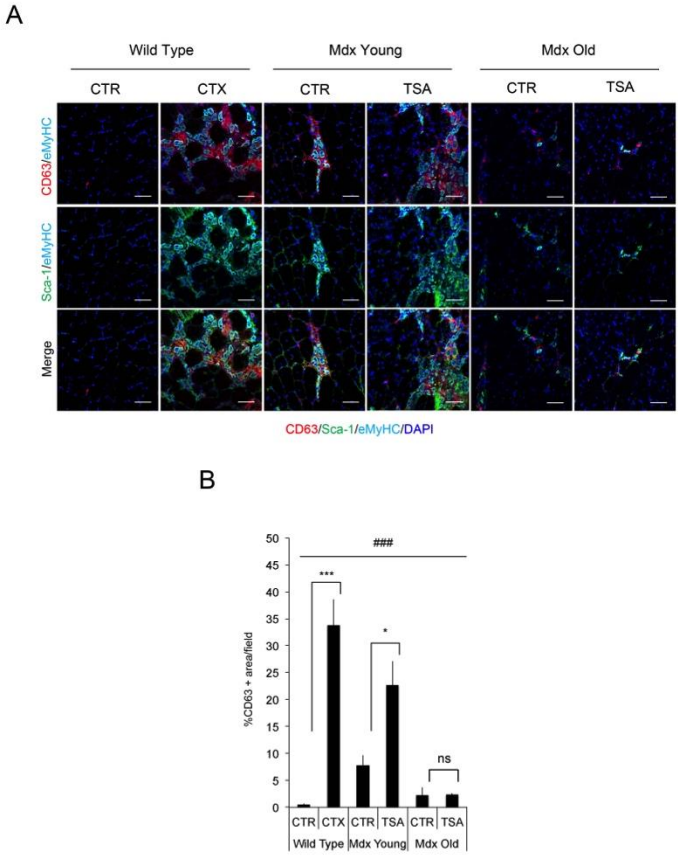

Figure 13 ***FAPs derived exosomes correlate with muscle regeneration.***
A) Representative images of immunofluorescence for CD63 (red), Sca-1 (green) and eMyHC (cyan) in muscle transversal sections of tibialis anterior from wild type mice (control –CTR- and cardiotoxin injured –CTX-), mdx young and old mice (control –CTR- and TSA treated). Scale bar = 50 μm. **B)** Graph relative to the quantification of CD63 positive signal showed in E. Star (*) indicates statistical analysis by t-test. *$p < 0.05$; *** $p < 0.001$. Hash (#) indicates statistical analysis by anova. ### $p < 0.001$. ns = not significant.

4.4 MicroRNAs (miRs) content of FAPs-derived exosomes mediate pro-myogenic effect of HDACi.

Exosomes are emerging as potent factors to transfer genetic informations from a cell to another cell. Indeed, exosomes are able to deliver functional mRNA, protein and microRNA (miRs) to recipient cells (EL Andaloussi et al., 2013).
Several works pointed on miRs as mediators of exosome-regulated different biological processes (Valadi et al., 2007; Hunter et al., 2008; Collino et al., 2010; Montecalvo et al., 2012; Vlassov et al., 2012; Nakamura et al., 2015; Fry et al., 2017).
Starting from the evidence about exosomes role in the cross-talk between FAPs and MuSCs, we analyzed whether miRs content of dystrophic FAPs-derived exosomes contribute to their ability to improve MuSCs activity. Therefore, we first determined whether FAP-derived exosomes could transfer RNA to MuSCs, by using fluorescent acridine orange (AO) - a specific nucleic acid staining. AO labeled FAPs-derived exosomes were incubated with freshly isolated MuSCs. Confocal microscopy analysis revealed AO-labeled intracellular RNA red spots inside recipient MuSCs, within and outside the nuclear membrane, confirming the ability of RNA transfer from FAPs and MuSCs through exosomes (Figure 14A).
In our previous studies, we described that in a permissive regenerative environment HDACi treatment enhances the ability of FAPs to influence MuSCs differentiation. We, also, demonstrated that HDACi extensively change the miRs expression pattern in FAPs from young mdx muscles, in particular up regulating the expression of myomiRs, such as miR-1, miR-133 and miR-206 (Saccone et al., 2014). Therefore, we speculated that the treatment with HDACi up-regulates miRs in exosomes released by FAPs, and this cargo is functional for the activity of FAPs on MuSCs. To test this hypothesis, we investigated the functional impact on muscle regeneration blocking miR biogenesis in treated FAPs. We

performed a co-culture experiment between HDACi-treated dystrophic FAPs and untreated dystrophic MuSCs. FAPs were, prior to co-culture, transfected with siRNA of Drosha (Drosha siRNA), the RNA-specific endoribonuclease required for miRs maturation, in order to inhibit miRs biogenesis. SiRNA efficiently down-regulated Drosha expression (by more than 90%) in FAPs (Figure 14B) and this event drastically reduced the ability of TSA-treated FAPs to enhance MuSC-mediated formation of multinucleated myotubes in transwell co-culture (Figure 14C and D), supporting the fundamental role of miRs in this communication.

To further shore up our hypothesis, we determined the identity of miRs within HDACi-treated FAPs, by performing a Taqman-based miRs expression microarray from exosomes isolated from the serum free media of FAPs derived by mdx mice treated for 15 days with TSA or control vehicle (CTR). This analysis revealed several miRs up-regulated in exosomes from TSA-treated mdx mice and we annotated the top 14 miRs significantly up-regulated (Figure 14E and F). Among them there are miRs that have been previously implicated in muscle processes and development, such as miR-449a, miR-30a, miR-494, miR-29a and miR-206 (Greco et al., 2009; Wang et al., 2012; Yamamoto et al., 2012; Wang, 2013; Guess et al., 2015; Nakamura et al., 2015). By the Ingenuity Pathway Analysis (IPA) we revealed number of regulatory pathways potentially affected by these 14 miRs and implicated in the control of MuSCs (Figure 14G). Moreover, when we performed IPA analysis on MuSCs, using RNAseq data generated from MuSCs isolated from mdx treated with TSA versus control vehicle, we found that at least 3 top activated pathways – Notch, JAK-STAT and TGFbeta - coincided with those predicted from up-regulated miRs of exosomes from FAPs of TSA-treated mdx mice (Figure 14H).

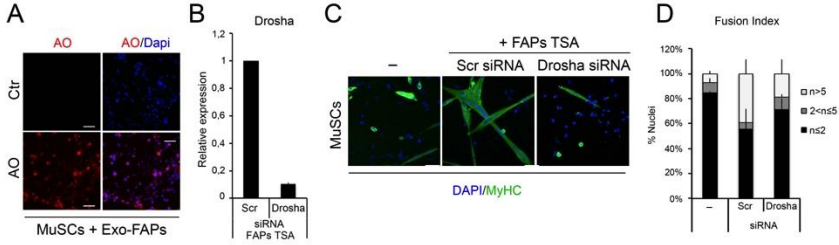

E

miR	Fold	P-value
miR-542-5p	2,06	0,007832466
miR-449a-5p	2,06	8,35409E-05
miR-342-3p	2,28	0,047153246
miR-320-3p	2,34	0,046067934
miR-192-5p	3,87	0,004641619
miR-423-5p	3,92	0,003867134
miR-376a-3p	3,94	0,007911342
miR-145a-5p	3,94	0,005581533
miR-224-5p	4,70	0,032604417
miR-30a-5p	4,82	0,03590865
miR-494-3p	7,93	0,000907818
miR-29a-3p	8,31	9,68344E-06
miR-7b-5p	9,78	0,008945472
miR-206-3p	17,06	0,000103942

F

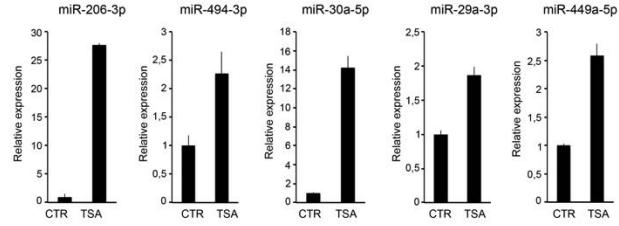

G

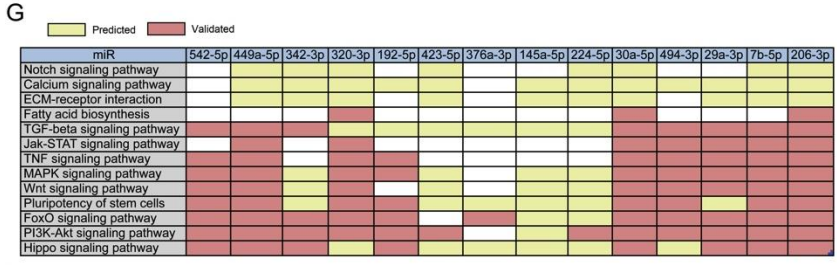

H

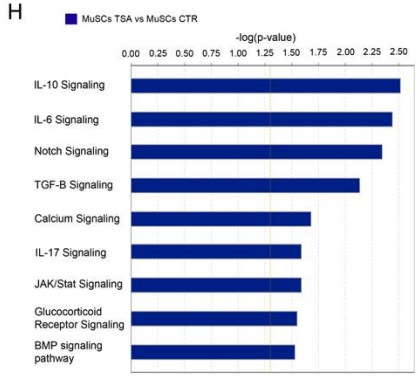

Figure 14 ***FAPs derived exosomes isolated from HDACi treated mdx mice contain miRs implicated in muscle regeneration.***
A) MuSCs uptake of RNA from FAPs-derived exosomes (Exo-FAPs). Exosomes harvested from FAPs donor cells were stained with Acridine Orange fluorescent dye (AO- red signal) or not (Ctr) and incubated with MuSCs. Nuclei were counterstained with DAPI (blue). Scale bar = 50 μm. **B)** Graph showing the relative expression of Drosha in FAPs from mdx mice treated with TSA after Drosha down-regulation by siRNA.**C)** Representative images of myogenic differentiation of MuSCs assessed by immunostaining for MyHC (green). Nuclei were counterstained with DAPI (blue). MuSCs were cultured alone (-) or in transwell co-culture with FAPs isolated from TSA treated mdx, treated with scramble (Scr siRNA) or Drosha siRNA (Drosha siRNA). Scale bar = 50 μm. **D)** Graph showing the fusion index of MuSCs in the conditions described in A. n<2 indicates the percentage of nuclei that were $MyHC^-$ or $MyHC^+$ in mononucleated myotubes. 2 <n< 5 indicates the % of nuclei that were $MyHC^+$ inside myotubes containing between 2 and 5 nuclei. n>5 indicates the % of nuclei that were $MyHC^+$ inside myotubes containing more than 5 nuclei. **E)** Table representing a manually assembled list of microRNAs revealed by microarray analysis and statistically induced by TSA in FAPs-derived exosomes. **F)** Graphs showing the relative expression of microRNAs resulted up-regulated in Exosomes from FAPs by TSA treatment. **G)** Table representing the Pathway Analysis of TSA upregulated miRs induced in FAPs-derived exosomes based on their predicted (shown in yellow) or already validated (in red) targets. **H)** Ingenuity Pathway Analysis of canonical pathways found significatively modulated in MuSCs TSA versus MuSCs CTR.

Interestingly, the most up-regulated miR in treated FAPs-derived exosomes was the myomiR miR-206 (17.06 fold). MiR-206 is involved in different processes that regulate muscle regeneration (Ma et al., 2015), and could be used as biomarker for the diagnosis of DMD (Cacchiarelli et al., 2011). Moreover, we recently demonstrated that miR-206 is part of a HDACi-activated network in dystrophic FAPs, that induces their ability to promote muscle regeneration leading to an improvement of muscle morphology and activity in mdx mice (Giordani et al., 2014; Saccone et al., 2014). MiR-206 is indeed modulate during DMD progression and after HDACi treatment. By *in situ* hybridization analysis of muscle biopsies from DMD patients at various ages (1, 4 and 9 years old) we revealed increased levels

of interstitial miR-206 (Violet signal), as compared to control biopsies (from non DMD boys), with a progressive reduction along with the disease progression that coincided with the exhaustion of the regenerative activity (eMyHC stainig) and the accumulation of fibrotic scars (Masson's Trichrome) (Figure 15A-F). The same pattern could be observed in mdx mice, in which an abundant miR-206 signal (Violet) was detected in the interstitium of tibialis anterior muscles, overlapping with the immunofluorescence staining of the FAP's marker Sca-1 (Green) (Figure 15G). Of note, treatment of young mdx mice with TSA, which promotes regeneration and inhibits fibrosis, increased the amount of interstitial miR-206 signal associated with Sca-1 staining (Figure 15H). To confirm the connection of miR-206 with DMD progression and the pharmacological effects of HDACi, we performed an analysis on miR-206 expression in exosomes isolated from unperturbed muscles and from treated or untreated dystrophic muscles at different ages. By qPCR, we verified that miR-206 increases in exosomes of young dystrophic muscles compared to unperturbed mice (WT), and the HDACi treatment further enhances its expression. No modulation of miR-206 expression was observed in old treated or untreated mice (Figure 15I).

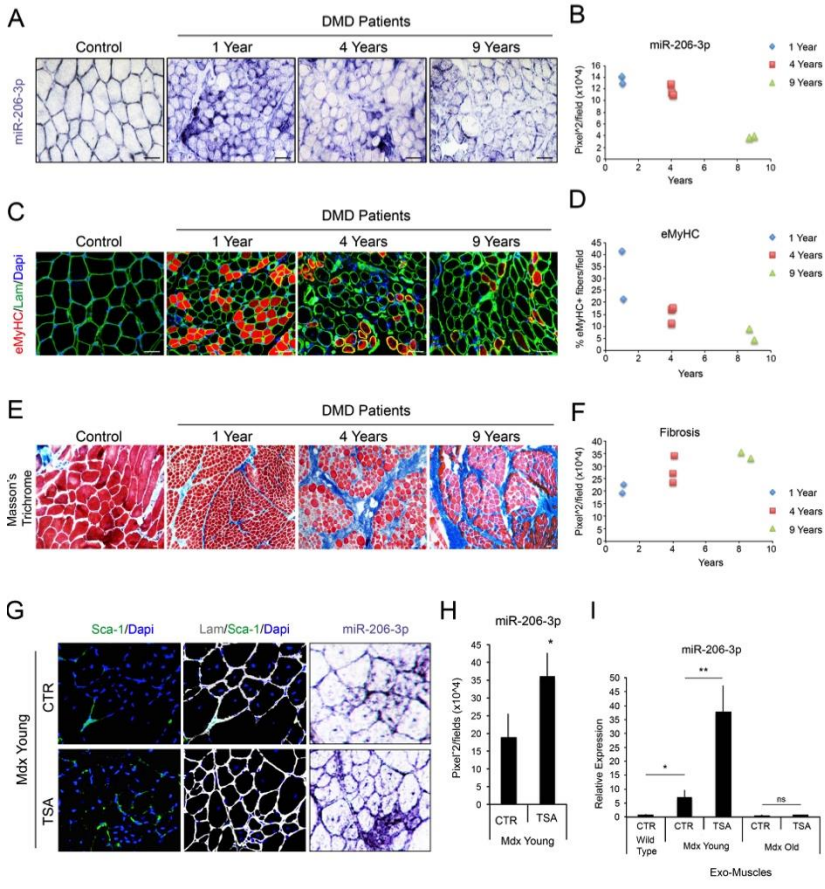

Figure 15 ***MiR-206-3p correlate with muscle regeneration and DMD progression.***
A) Representative images of miR-206-3p (violet) immunohistochemistry in vastus medialis biopsies of Control and DMD patients at different ages: 1 year, 4 years and 9 years old. Scale bar = 50 µm. **B)** Graph representing the distribution of miR-206-3p violet area quantification measured as pixel^2/field relative to DMD patients' age: DMD patients of 1 year old n=2; DMD patients of 4 years old n=3, DMD patients of 9 years old n=2. **C)** Representative images of immunofluorescence for eMyHC (red) and Laminin (green) in vastus medialis biopsies of not DMD patients Control and DMD patients at different ages: 1 year, 4 years and 9 years old. Nuclei were counterstained with DAPI (blue). Scale bar = 50 µm. **D)** Graph showing the distribution of eMyHC positive fibers percentage of DMD patients at different ages: DMD patients of 1years old n=2; DMD patients of 4 years old

n=3, DMD patients of 9 years old n=2. **E)** Representative images of Masson's Trichrome staining in vastus medialis biopsies of Control and DMD patients at different ages: 1 year, 4 years and 9 years old. Nuclei were counterstained with DAPI (blue). Scale bar = 50 μm. **F)** Graph showing the distribution of fibrosis area quantification, measured as pixel^2/field, relative to DMD patients' age: DMD patients of 2 years old n=2; DMD patients of 4 years old n=3, DMD patients of 9 years old n=2. **G)** Representative images of Sca-1 (green), Laminin (white) and DAPI (blue) immunofluorescence (left and middle panels) and of miR-206-3p (violet) immunohistochemistry (right panel) in transversal sections of Tibialis Anterior (TA) of young mdx mice (CTR) and after TSA treatment (TSA). **H)** Graph showing the quantifications of miR-206-3p violet area measured as pixel^2/field relative to the experimental points indicated in K (n=3). Statistical significance tested by t-test. Star (*) indicates statistical analysis by t-test. * $p < 0.05$. **I)** Graph representing the miR-206 relative expression in exosomes isolated from muscle interstitium of tibialis anterior from wild type mice (CTR), mdx young and old mice (control –CTR- and TSA treated). Star (*) indicates statistical analysis by t-test. *$p < 0.05$; ** $p < 0.01$; ns = not significant.

4.5 MiR-206 in exosomes isolated from FAPs of HDACi-treated dystrophic muscles is required to promote MuSCs activation, expansion and differentation.

To evaluate the impact of miR-206 on FAPs-derived exosomes ability to enhance MuSC-mediated formation of multinucleated myofibers, we simulated co-culture experiment adding exosomes from FAPs directly on MuSCs culture. We used exosomes purified from TSA-treated dystrophic FAPs and transfected with antagomiR-206 (TSA A-206) or vehicle (TSA). By immunofluorescence for MyHC (Green), we tested their ability to promote MuSC-mediated formation of multinucleated myotubes. Exosomes purified from FAPs transfected with antagomiR-206 (TSA A-206) showed a reduced ability to promote MuSC-mediated formation of multinucleated myotubes, as compared to exosomes purified from FAPs isolated from vehicle (TSA), as well as to FAPs from untreated (CTR) mdx mice (Figure 16A-C). Thus, miR-206 is an essential

component of the FAP-derived exosomes that support MuSCs differentiation ability *ex vivo*.

To gain mechanistic insights into the pro-myogenic activity of exosomes derived from FAPs of HDACi-treated dystrophic muscles, we searched for putative target genes of miR-206 that matched with down regulated genes in our RNA-seq datasets obtained from MuSCs of TSA-treated mdx mice (Figure 16D). A downstream analysis was carried only for miR-206 targets that have been already annotated or predicted with high confidence. Ingenuity pathway analysis (IPA) revealed a potential effect of miR-206 on various signaling pathways involved into muscle development and disease, including utrophin (UTRN), Pax7 and Notch3 (Rosenberg et al., 2006; Chen et al., 2010; Cacchiarelli et al., 2010; Gagan et al., 2012; Amirouche et al., 2014).

We decided to focus on miR-206 regulation of Notch3, as negative regulator of MuSCs differentiation, as previous works demonstrated that miR-206 down-regulation of Notch3 promotes MuSCs differentiation (Gagan et al., 2012). While both Notch3 and Notch1 transcripts were reduced in MuSCs isolated from mdx mice treated with TSA, we observed a selective down regulation of Notch3 transcripts in MuSCs isolated from untreated mdx mice and cultured with exosomes derived from FAPs of TSA-treated mdx mice (Figure 16D and E).

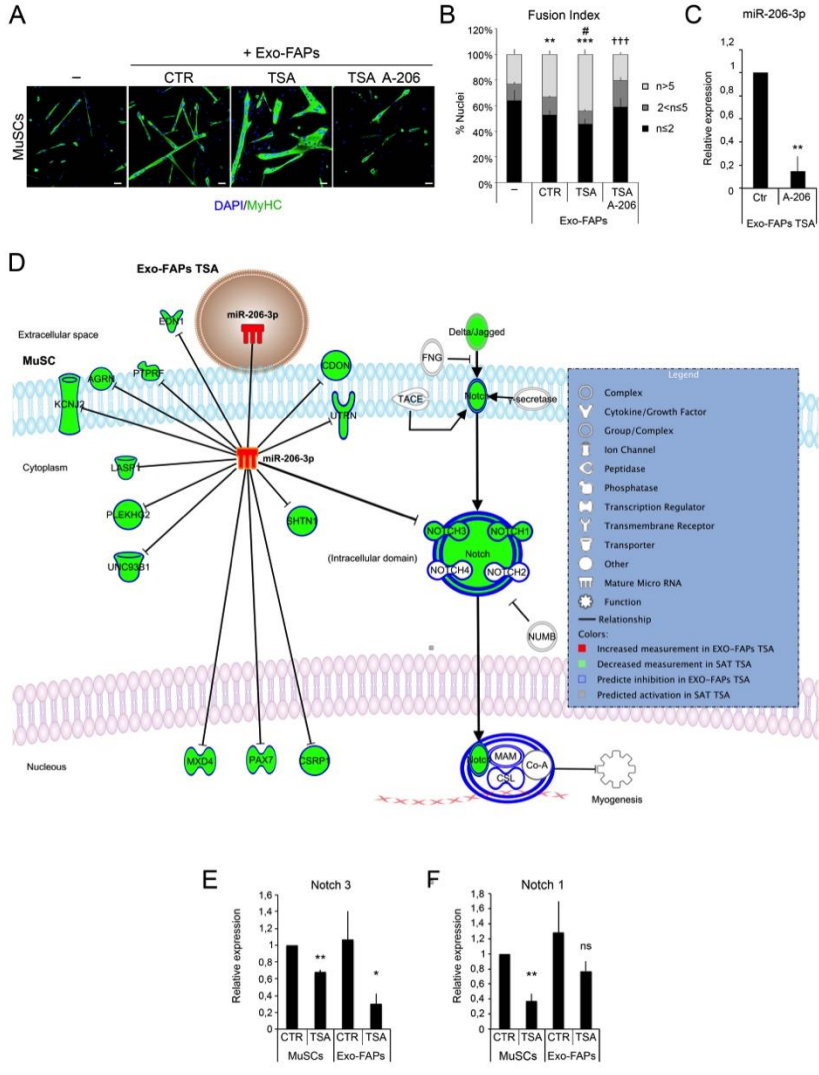

Figure 16 ***Biological effect of exosomal miR-206-3p from HDACi treated FAPs on MuSCs differentiation and its targets.***

A) Representative images of myogenic differentiation of MuSCs assessed by immunostaining for MyHC (green). Nuclei were counterstained with DAPI (blue). MuSCs were cultured alone (-) or with exosomes (Exo FAPs) isolated from FAPs *in vivo* exposed or not to TSA (CTR and TSA) and subsequently treated with antagomiR-206 (TSA A-206). Scale bar = 50 µm. **B)** Graph showing the fusion index of MuSCs in the condition described in

A. n<2 indicates the percentage of nuclei that were $MyHC^-$ or $MyHC^+$ in mononucleated myotubes. 2 <n< 5 indicates the % of nuclei that were $MyHC^+$ inside myotubes containing between 2 and 5 nuclei. n>5 indicates the % of nuclei that were $MyHC^+$ inside myotubes containing more than 5 nuclei. Star (*) indicates statistical analysis by t-test relative to MuSCs cultured alone (-). Star (*) means significance compared to MuSCs alone, **p < 0.01, ***p>0,001; hash (#) means significance compared to Exo-FAPs CTR, #p<0,05; cross (†) indicates significance compared to Exo-FAPs TSA, †††p<0,001. **C)** Graph showing the relative amount of miR-206-3p in Exosomes isolated from FAPs of mdx mice treated with TSA (Exo-FAPs TSA): control (Ctr) or transfected with antagomiR-206 (A-206). Star (*) indicates statistical analysis by t-test; **p < 0.01. **D)** Cartoon showing the putative activity of miR-206-3p released in exosomes from FAPs exposed to TSA on MuSCs targets. Ingenuity Pathway Analysis intersecting RNAseq data from MuSCs-TSA with Exo-FAPs TSA microarray generated the Cartoon. Notch3 signaling modulation is highlighted on the right. **E)** Graph relative to Notch3 expression in MuSCs isolated from mdx vehicle treated (CTR) and from TSA daily treated mdx mice and to exosomes from FAPs (Exo-FAPs) isolated from vehicle (CTR) and TSA daily treated mdx animals. Star (*) indicates statistical analysis by t-test relative to mdx vehicle treated mdx mice (CTR); *p<0,05; **p < 0.01. **F)** Graph relative to Notch1 expression in MuSCs isolated from mdx vehicle treated (CTR) and from TSA daily treated mdx mice and to exosomes from FAPs (Exo-FAPs) isolated from vehicle (CTR) and TSA daily treated mdx animals. Star (*) indicates statistical analysis by t-test relative to mdx vehicle treated mdx mice (CTR); **p < 0.01. ns = not significant.

In keeping with the opposite roles of Notch members in MuSCs activation (Kitamoto and Hanaoka, 2010), we reasoned that selective down regulation of Notch3 by exosomal miR-206 could promote MuSCs activation and self-renewal. To investigate this hypothesis, we evaluated the effect of FAP-derived exosomes from HDACi-treated or control-treated mdx mice on MuSCs within single fibers isolated from WT mice. Freshly isolated single muscle fibers from tibialis anterior, extensor digitorum longus, gastrocnemius and soleus of C57BL6J mice were incubated with FAP-derived exosomes (Exo-FAPs) or whole conditioned media (MEDIA-FAPs), and their effect on MuSCs was evaluated by monitoring the expression of Pax7 (Green), MyoD (Red) and DNA synthesis

(EdU incorporation-Cyan). In this experimental setting, the uptake of FAP-derived exosomes by MuSCs from single fibers was first confirmed by staining of lipidic dye PKH-67 used on purified vesicles (Figure 17A). The whole supernatant derived from FAPs of control-treated mdx mice increased the number of Pax7+/MyoD+ MuSCs that exhibited enhanced DNA synthesis (Edu+) and could be therefore considered activated, "transiently amplifying" MuSCs (Zammit et al., 2004). Moreover, the whole supernatant derived from FAPs of TSA-treated mdx mice could further increase this effect. While a drastic reduction in the number of quiescent (Pax7+ MyoD-) and differentiation-committed (Pax7- MyoD+) MuSCs was observed upon incubation with the whole supernatant of FAPs isolated from control-treated mdx mice and pre-exposed to GW4869, the number of Pax7+/MyoD+ MuSCs with high DNA synthesis (Edu+) was not altered in these conditions (Figure 17B-D). By contrast, GW4869 treatment of FAPs from TSA-treated mdx mice drastically reduced the ability of the whole supernatant to increase all MuSC populations as well as their proliferation (Figure 17B-D). This result indicates that the ability of FAPs from mdx mice to support MuSCs activation and differentiation, but not expansion of Pax7+/MyoD+ MuSCs, relies on exosomal factors, while the ability of FAPs from HDACi-treated mdx mice to promote expansion of MuSCs entirely depends on exosomes. Indeed, exosomes from FAPs of TSA-treated (but not from control-treated) mdx mice increased the number of Pax7+/MyoD+ MuSCs (Figure 17B-D). We then investigated the relative contribution of exosomal miR-206 in mediating the ability of FAPs from TSA-treated mdx mice to support MuSC activation, expansion and differentiation, by transfecting miR-206 antagomiR in FAPs 24 hours prior to the purification of the exosomes. This blockade of miR-206 could completely abrogate FAP ability to support MuSCs, pointing to a central role of exosomal miR-206 in mediating HDACi ability to promote functional interactions between dystrophic FAPs and MuSCs (Figure 17B-D).

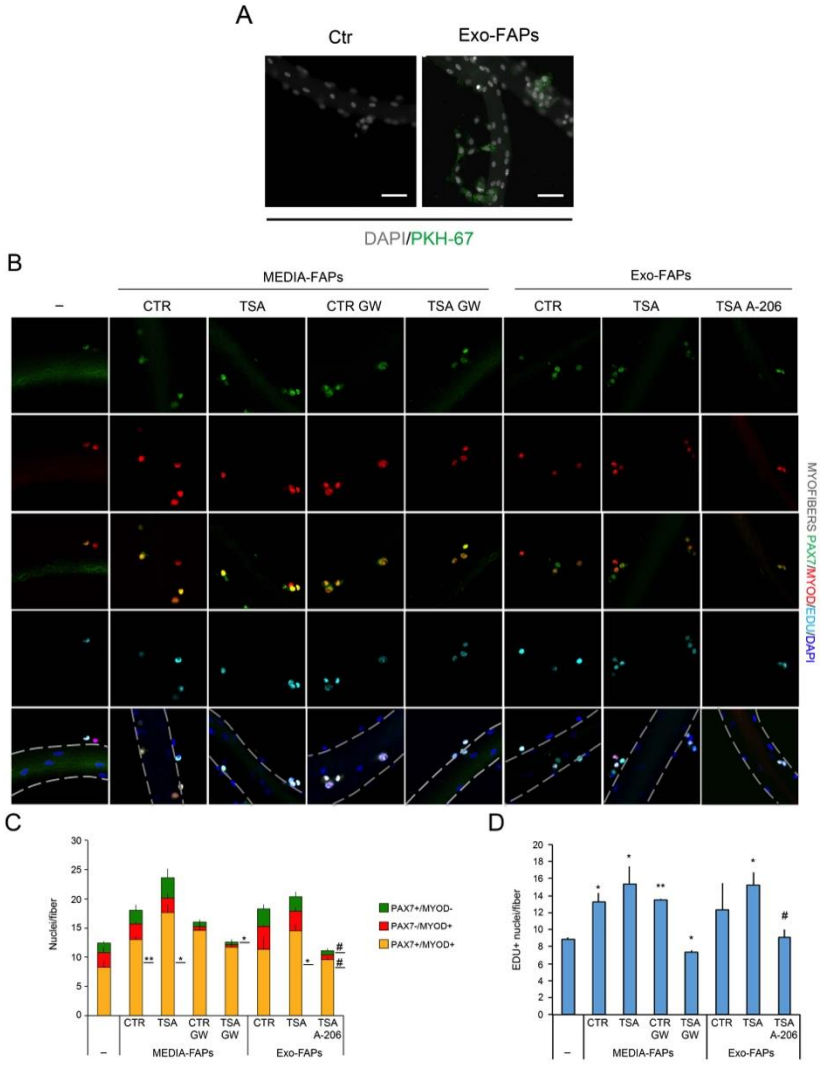

Figure 17 ***Exosomal miR-206-3p of HDACi treated mdx mice promotes expansion and asymmetrical division of MuSCs.***
A) Representative images showing myofibers cultured alone (Ctr) or with exosomes isolated from FAPs (Exo-FAPs) and stained with PKH-67 (green). Scale bar = 50μm. **B)** From left to right: representative images of myofibers cultured for 24 hours alone (-) or with conditioned media of FAPs that were previously exposed or not to TSA and GW4869 (MEDIA-FAPs) or

exosomes (Exo-FAPs) collected from FAPs exposed or not to TSA *in vivo* (CTR and TSA) and transfected with antagomiR-206 (TSA A-206). Myofibers have been stained for immunofluorescence with αPax7 (green), αMyoD (red), EDU (cyan). Nuclei were counterstained with DAPI (blue). **C)** Graph showing the average of nuclei positive for Pax7 (green), MyoD (red) or both (yellow) for single fiber in the experimental points indicated in B. Star (*) indicates statistical analysis by t-test relative to myofibers cultured alone (-). * $p < 0.05$, ** $p < 0.01$. Hash (#) indicates statistical analysis t-test relative to Exo-FAPs TSA. # $p < 0.05$. **D)** Graph showing the average of EDU positive nuclei (cyan) for single fiber in the experimental points indicated in F. Statistical analysis is shown as described in C.

4.6 Exosomal miR-206 is required to promote compensatory regeneration and reduce fibrosis, but not inflammation, in dystrophic muscles.

We finally investigated whether FAP-derived exosomes (Exo-FAPs) could promote muscle regeneration *in vivo*, within the context of the mouse model of DMD – the mdx mice – in which HDACi exert beneficial effects, by promoting compensatory regeneration, and by reducing fibrosis and inflammation (Minetti et al., 2006). As we sought to evaluate to what extent these effects are accounted by FAP-derived exosomes, we compared the ability to stimulate regeneration, reduce fibrosis and inflammation in mdx muscles of systemic exposure to TSA (or vehicle control), as administered via daily intra-peritoneal injection, versus intramuscular injection of exosomes purified from FAPs isolated from mdx mice that were previously treated with TSA (Exo-FAPs TSA) or vehicle (Exo-FAPs CTR). The exosome injection was repeated every 7 days for 21 days, a timeframe that we found compatible to quantify the histological parameters of productive regeneration, fibrosis and inflammation, and is equivalent to the time of systemic exposure to TSA. We first verified the successful injection of Exo-FAPs, with PKH-67 staining, as assessed by flow cytometry. For this assay, we exploited the ability of CytoFLEX to detect nano-

molecules. Using a mixture of non-fluorescent silica beads and fluorescent (green) latex beads with sizes ranging from 110 nm to 1300 nm, we revealed PKH-67 positive staining of about 67% of exosomes, prior to their injection (Figure 18A). Using this procedure we could evaluate the persistence of injected exosomes, by detection in the box of flow chart of the green signal in transplanted muscles (Figure 18B).

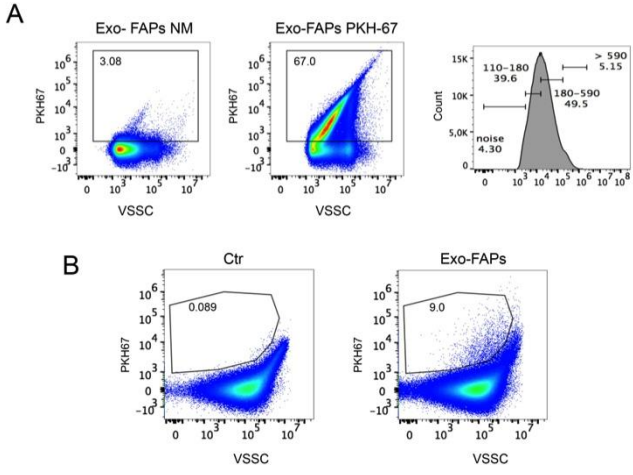

Figure 18 ***FAPs exosomes injection in mdx TA muscle.***
A) Flow cytometry analysis of exosomes isolated from FAPs and stained or not with PKH-67 lipidic dye. The left panel represents sample without PKH-67 staining (Exo-FAPs NM); middle panel shows sample stained with PKH67 dye (Exo-FAPs PKH-67); right panel shows the size of the PKH-67 positive Exosomes. **B)** Flow cytometry analysis of digested muscles previously injected with vehicle (Ctr) or with PKH67-labeled exosomes isolated from FAPs (Exo-FAPs). The left panel shows muscle injected with PBS. Right panel shows muscle injected with PKH-67 labeled exosomes.

Exo-FAPs TSA injected muscles showed an increase in both fibers caliber, as measured by cross sectional area (CSA), and embryonic-MyHC-positive myofibers (eMyHC-red), that were comparable to those produced by systemic delivery of TSA (Figure 19A-C). Likewise, we observed a comparable ability of

Exo-FAPs TSA intramuscular transplantation and systemic delivery of TSA to increase muscle fiber area fraction (MFAF), reduce fibrosis (Figure 19D-F) and inflammation (Figure 19G and H) in mdx muscles. A significant reduction of MPO-positive area (Red signal) similar to what calculated for mice daily treated with TSA, was observed in Tibialis anterior muscles of all animals (Figure 19G and H).
To evaluate the contribution of miR-206 to the effects of FAP-derived exosomes on mdx mice, FAPs isolated from TSA-treated mice were transfected with AntagomiR-206 (Exo-FAPs TSA A-206) prior to exosome isolation and injection into Tibialis Anterior of mdx mice. While exosomes isolated from FAPs+A206 showed a reduced ability to stimulate muscle regeneration (Figure 19A-C) and reduce fibrosis (Figure 19D-F), they could still decrease inflammation, indicating a selective contribution of miR-206 to promote regeneration and reduce fibrosis. By contrast, the anti-inflammatory effect of FAP-derived exosomes appear to be independent on miR-206 (Figure 19G and H).

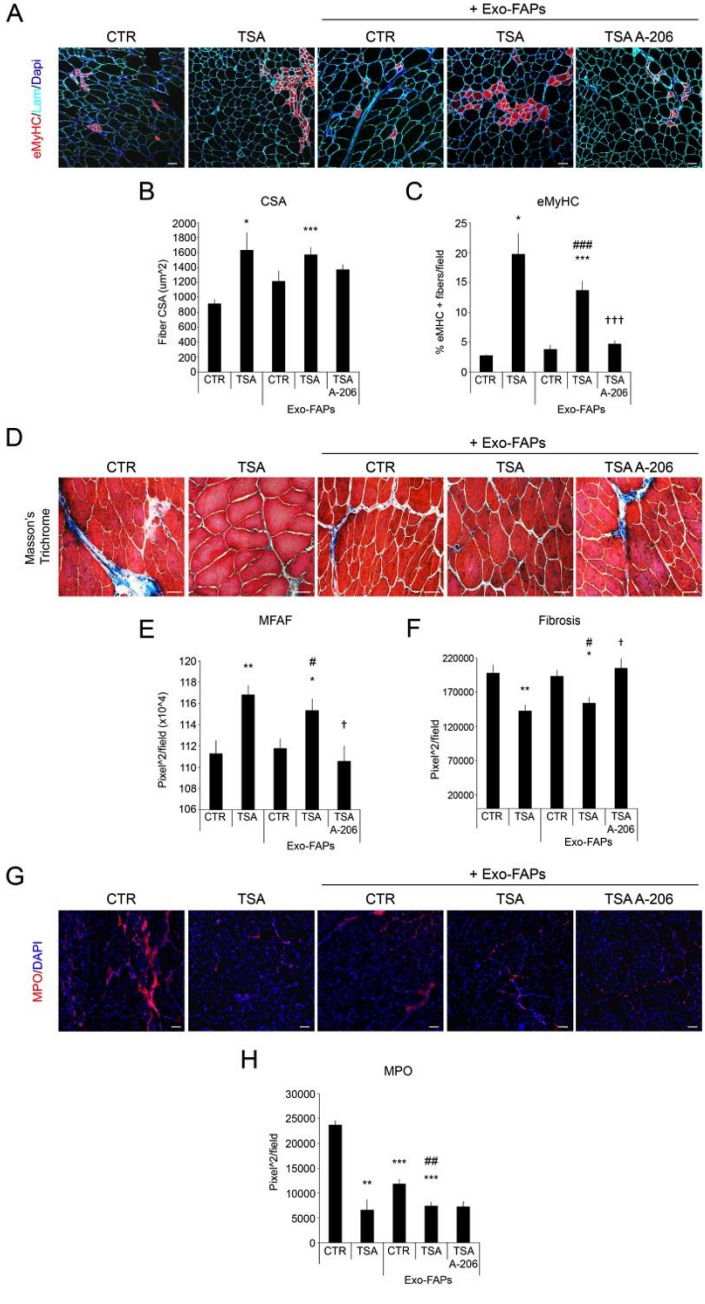
A
+ Exo-FAPs
CTR
TSA
CTR
TSA
TSA A-206
eMyHC/Lam/Dapi
B
CSA
Fiber CSA (um^2)
C
eMyHC
% eMHC + fibers/field
Exo-FAPs
D
Masson's Trichrome
E
MFAF
Pixel^2/field (x10^4)
F
Fibrosis
Pixel^2/field
G
MPO/DAPI
H
MPO
Pixel^2/field

Figure 19 ***FAPs derived exosomes improve muscle regeneration and inhibit fibrosis through miR-206-3p content.***
A-H) Stainings on Tibialis Anterior muscle transversal sections of 1.5 months old mdx mice (n=5 per group) treated daily for 21 days with intra-peritoneal injection of vehicle (CTR) or TSA, or once a week with intramuscular injections (Tibialis Anterior) of exosomes derived from FAPs (Exo-FAPs) exposed or not to TSA *in vivo* (Exo-FAPs CTR, Exo-FAPs TSA) and of Exo-FAPs TSA transfected with antagomiR-206 (TSA A-206). Exosomes were injected every seven days and sacrificed after 21 days of treatment. **A)** Representative images of immunofluorescence for embryonic myosin heavy chain (eMyHC-red) and laminin (Lam-cyan) stainings. Nuclei were counterstained with DAPI (blue). Scale bar = 50 μm. **B)** Graph showing the quantifications of cross-sectional area (CSA), measured as μm^2. Statistical significance tested by t-test. Star (*) means significance compared to CTR, *p < 0.01, ***p<0,001 n=5. **C)** Graph showing the quantifications of muscle regeneration (eMyHC), measured as percentage of eMyHC positive fibers/field. Statistical significance tested by t-test. Star (*) means significance compared to CTR, *p<0,05; ***p < 0.001; hash (#) means significance compared to Exo-FAPs CTR, ###p<0,001; cross (†) indicates significance compared to Exo-FAPs TSA †††p<0,001. n=5. **D)** Representative images of Masson's Trichrome staining. **E)** Graph showing the quantifications of muscle fiber area fraction (MFAF), measured as pixel^2/field. Statistical significance tested by t-test. Star (*) means significance compared to CTR, *p<0,05; **p < 0.01; hash (#) means significance compared to Exo-FAPs CTR, #p<0,05; cross (†) indicates significance compared to Exo-FAPs TSA †p<0,05 n=5. **F)** Graph showing the quantifications of fibrosis area, measured as pixel^2/field. Statistical significance tested by t-test. Star (*) means significance compared to CTR, *p<0,05, **p < 0.01; hash (#) means significance compared to Exo-FAPs CTR, #p<0,05; cross (†) indicates significance compared to Exo-FAPs TSA †p<0,05. n=5. **G)** Representative images of myeloperoxidase staining (MPO-red); Nuclei were counterstained with DAPI (blue). Scale bar = 50 μm. **H)** Graph showing the quantifications of inflammation (MPO), measured as pixel^2/field. Statistical significance tested by t-test. Star (*) means significance compared to CTR, **p < 0.01; ***p<0,001; while hash (#) means significance compared to Exo-FAPs CTR, ##p<0,01. n=5.

5. Discussion

The identification of mediators that coordinate the activities of the cellular components of the muscle stem cell niche could suggest novel selective strategies for DMD treatment, which aim to promote compensatory regeneration and eliminate the deposition of fibrotic and adipose tissue that typically compromises contractile activity and regenerative potential of muscles.

Several groups described a variety of soluble factors involved in the reciprocal functional interactions between the major cellular components of the muscle stem cell niche, such as inflammatory cytokines and growth factors; among them exosomes are emerging as powerful tool to transfer biochemical and genomic information from one cell type to another (Lee et al., 2012; Braicu et al., 2015; Iraci et al., 2016).

Hence, the exchange of exosomes content, consisting of proteins, mRNAs and miRs, allows the functional interactions between neighbor cells leading to an activation of different biological processes in the recipient cells. As such, the qualitative and quantitative content of exosomes appears as the major determinant of their biological activity.

In this study, we demonstrated the role of exosomes in mediating the interactions between FAPs and MuSCs during muscle regeneration and DMD.

Specifically, our findings highlighted that miR-206-enriched exosomes derived from FAPs of dystrophic muscles exposed to HDACi promote MuSCs activation and differentiation. Moreover, we showed that FAPs exosomes content mediates the HDACi beneficial effects *in vivo,* demonstrating, by intramuscular injections in mdx mice, the ability of FAPs derived exosomes to improve the compensatory regeneration, while inhibiting the fibrotic tissue deposition.

Previous works have shown the role of miRs content of exosomes on their ability to influence different processes such

as skeletal myogenesis (Choi et al., 2016) and fibrosis during muscle hypertrophy (Fry et al., 2017). The pro-regenerative and anti-fibrotic activities of miR-206 have been largely documented by previous studies (Ma et al., 2015). However, while these studies invariably indicated skeletal myofibers and MuSCs as source of miR-206, our study reveals HDACi-treated FAPs from dystrophic muscles as an additional cellular source of miR-206, raising important questions related to the function of miR-206 exchange through exosomes from FAPs to the major cellular source of miR-206 – the MuSCs. We propose that additional amounts of miR-206 from FAP-derived exosomes could correct the dysfunctional phenotype of MuSCs by normalizing intracellular miR-206, as also indicated by previous studies showing that transgenic expression of miR206 has beneficial effects in mdx mice (Liu et al., 2012).

Recent discoveries demonstrated that dystrophin is expressed in MuSCs, and dystrophin-deficient MuSCs loose the ability to divide asymmetrically and regenerate DMD muscles (Dumont et al., 2015; Chang et al., 2016) indicating that additional events downstream of dystrophin can be deregulated in DMD MuSCs. Among them, aberrant HDAC-mediated repression of miR-206 (Colussi et al., 2008; Cacchiarelli et al., 2010) could be compensated by FAP-derived exosomal miR-206 and therefore restore MuSCs ability to regenerate dystrophic muscles.

In addition, we elucidated the ability of FAP-derived exosomes to deliver to MuSCs a cargo of other miRs and proteins, suggesting the possibility that the effect of exosomes cargo on MuSCs, *ex vivo,* and on regeneration of dystrophic muscles, *in vivo,* is due to a combinatorial effect of the whole exosomal content. The observation of miR206 requirement, *in vivo,* for muscle regeneration and for anti-fibrotic activities of FAP-derived exosomes, but not for their anti-inflammatory effects, confirms that the whole cargo (miRs and proteins) of exosomes isolated from FAPs is necessary to mediate the HDACi beneficial consequences. In particular, other miRs or proteins

can mediate the anti-inflammatory activity of exosomes from HDACi-treated FAPs.

We speculate that in FAPs derived exosomes exposed to HDACi treatment exist a well-regulated combination of miRs that exerts beneficial effect to counteract DMD progression and the lack of just one component of this mix of miRs leads to a reduction or also totally absence of their effects *ex vivo* and *in vivo*.

Further studies will be necessary to understand whether systemically injections of exosomes could reach the damaged muscles exerting their beneficial effects and how HDACi are able to regulate exosomal biogenesis and content. These findings will allow the design of potential selective treatment for DMD using FAPs-derived exosomes.

Overall, our study provides the first evidence that FAP-derived exosomes mediate functional interactions with MuSCs, and that exosomal miR content could be pharmacologically modified (e.g. by HDACi) for therapeutic purpose for DMD.

6. Materials and Methods

6.1 Animals and *in vivo* treatments

Mice were bred, handled and maintained according to the standard animal facility procedures and the internal Animal Research Ethical Committee according to the Italian Ministry of Health approved all experimental protocols and the ethic committee of the Fondazione Santa Lucia (FSL) approved protocols.
C57/BL6 mice were provided by the Core Structure of the EMMA (European *Mouse* Mutant Archive, Monterotondo, Rome), C57Bl6 mdx mice were purchased from Jackson Laboratories. All mice used for *in vitro* and *ex vivo* experiments including FAPs-derived exosome transplant. Note that the term of "young" is refereed to C57BL6/mdx mice 6/8 weeks old while the term of "old" is refereed C57BL6/mdx mice 9 months old.
Animals were used at the specified age and treated for the indicated periods with daily intra peritoneal injections of Trichostatin A, TSA (0.6 mg/kg/day; #T8552, Sigma), dissolved in in phospate-saline solution or in phospate-saline alone as vehicle control (CTR). Muscle injury was performed by intramuscular injection in Tibliais Anterior (TA) of Cardiotoxin -CTX- (10 μM, 10 mg/mL) (#L8102, Lotaxan Valence, France, http://www.latoxan.com), 3 days before mice sacrifice.
FAPs-derived exosomes at a final concentration of 10 μg in 20 μL of PBS1x (0.5μg/μl) (#14190-1444, Gibco by life technologies) and its vehicle of control (20 μl PBS1x) were injected 3 times in left TA of young C57BL6/mdx mice: every 7 days for 21 days.

6.2 Human Samples

Human bioptic samples were kindly provided by Dr. Bertini and Dr. D'Amico (Ospedale Bambino Gesù, Rome) and thanks to the parents' informed consent it was possible to use samples for research purposes. We used 10 μm transversal sections isolated from *vastus medialis* of DMD boys at different ages: 1 year old (n=2), 4 years old (n=3), 9 years old (n=2) and we compared with a vastus medialis section of control (no DMD) samples.

6.3 Histology and in situ hybridization

The Tibialis anterior muscles were snap frozen in liquid nitrogen-cooled isopentane and then cut transversally with a thickness of 7 μm.
For Masson Trichrome staining to analyze fibrotic tissue, muscle cryo-sections were fixed for 20' at 56°C in Bouin's Solution (#HT10132, Sigma) and then stained in Working Weigert's Iron Hematoxilin solution for 5 min (#HT1079, Sigma), washed in running tap water for 5 min and stained in Biebrich Scarlet-Acid Fucsin for 5 min (#HT151, Sigma). Sections were rinsed in de-ionized water and re-fixed in freshly made Phosphomolybdic/Phosphotungstic (1:1) acid solution for 8 min (#HT153, #HT152, Sigma), and then they are stained in Aniline Blue solution for 5 min (#HT154, Sigma) and in acid acetic 1% for 2 min (#27221, Sigma). The slides were dehydratated in ethanol (#02860, Sigma) and xilene (#X1040, Sigma) and mounted with EUKITT (#03989, Sigma), then visualized using a Nikon Eclipse 90i: collagen fibers are stained in blue, the nuclei stained in black and the muscle tissue is stained in red. miR *in situ* hybridization was performed as described by Pena (2009) in formaldehyde and carbodiimide (EDC)-fixed TA cryo-sections (0,16M 90 min at RT, #25952-53-8, Merck KGaA). After washes with 0,2% glycine (#G8898,

Sigma) and TBS, cryo-sections were acetylated using 0,1 M triethanolamine and 0,25% acetic anhydride for 25 min at RT (respectively #90275, #A6404, Sigma). This steps are followed by a pre-hybridization using 2X of SSC, 25% formamide (#F9037, Sigma); 0,2% Triton (#X100, Sigma) 30 min at RT and by the over night hybridization at 4°C with the has-miR206 probe (10 pmol, #18100-01, exiqon) dissolved in a solution of 50% formamide, 250µg/ml tRNA (#R1753, Sigma), 200µg/ml SSDNA (#D7656, Sigma), 10% dextran sulphate (#D8906, Sigma) and 2X SSC. The hybridization was followed by specific washes with SSC to eliminate non specific binding of probe (5X SSC 5min at RT, 1X SSC 15 min at 45°C, 2%BSA in 0,2X SSC 15min at 4°C, 2X SSC 5min at RT, TNbuffer 10 min at RT and TNT buffer 15' at RT) and by the incubation of cryo-section using anti-digoxigenin-ap fab fragments (1/100, #11093274910, Roche) dissolved in TNbuffer for 2 hours at RT. To reveal the miR probe specific binding cryo-sections, covered from light, were incubating over night at 4°C with 0,375 mg/ml of NBT and 0,188 mg/ml BCIP dissolved in a solution of TMNbuffer (respectively #11383213001 and #11383221001, Roche).
TNbuffer is composed of 0,1 M Tris-HCL (#T1503, Sigma) and 0,15 M Nacl (#S3014, Sigma) at pH 7,5; TNTbuffer is TNbuffer with 0,1% Tween (#P1379, Sigma) while TMNbuffer is composed of 0,1 M Tris-HCL, 0,005M $MgCl_2$ (#M8366, Sigma), 0,5 M NaCl and 2mM of Levamisole (#L9756, Sigma).

6.4 Isolation of FAPs and Satellite cells (MuSCs).

FAP cells were isolated as $TER119^{neg}/CD45^{neg}/CD31^{neg}/a7INTEGRIN^{neg}/SCA\text{-}1^{pos}$ cells, MuSCs were isolated as $TER119^{neg}/CD45^{neg}/CD31^{neg}/a7INTEGRIN^{pos}/SCA\text{-}1^{neg}$ cells using a procedure described in Mozzetta et al. (2013).
Briefly, hind limb muscles for each mouse were minced and put into a 15 mL tube containing 4 mL of HBSS (#24020-091, GIBCO) BSA (0.2%, #A7030, Sigma) and
10 Units/ml Penicillin and 10 µg/ml streptomycin (P/S), 2 mg/ml Collagenase A (#10103586001, Roche), 2.4U/ml Dispase

II (#04942078001, Roche), DNaseI 10 mg/ml (#11284932001, Roche) at 37^0C under gentle agitation for 1hr and 30 min.
The supernatants were filtered through a 100um, 70um and 40um cell strainers (#08-771-19, #08-771-2, #08-771-1, BD Falcon). Cells were spun for 15 min at 300 g at 4°C, the pellets were re-suspended in 0.5 mL of HBSS 1x containing DNase I and incubated with antibodies on ice for 30 min. The following antibodies were used: CD45-eFluor 450 (1/50, #48-0451-82, Leukocyte Common Antigen, Ly-5, eBiosciences), CD31-eFluor 450 (1/50, PECAM-1, #48-0311-82, eBioscience), TER-119- eFluor 450 (1/50, clone TER-119, #48-5921-82, eBiosciences), Sca1-FITC (1/50, Ly-6A/E FITC, clone D7, #11-5981-82, eBioscience), Itga7-649 (1/500, AbLab #67-0010-01). HBSS was added and cells were spun for 5 min at 300 g at 4^0C to stop the reaction. The cells were re-suspended in HBSS containing 1% DNaseI and were isolated based on size, granulosity and fluorophores levels using a FACS MoFlo HS Cell Sorter Dako Cytomation (BD) and analyzed using FlowJo.

6.5 Cell culture

MuSCs and FAPs were cultured after sorting directly in culture media: for MuSCs: 20% FBS (#16000044, GIBCO), 10% HS (#26050-070, GIBCO), 1% Penicillin-Streptomycin (#15140, GIBCO), 1% Chicken Embryo Extract (CEE, #CE-650-F, Seralab) in DMEM + Pyruvate (#41966, GIBCO) and for FAPs: BIOAMF-2 (Biological Industries). MuSCs were plated at low density on regular cell culture dishes coated with Gelatin 0.1% (#07903, Stemcell).
FAP cells were cultured in Bioamf-2 at high density (200.000 cells in 10 cm-well plate) for exosome isolation, at low density: 40000 or 10000 cells respectively in 6 or 24 well dishes for co-culture experiments.
To isolate exosomes, FAP cells reached 80-90% of confluence then, the medium was replaced with DMEM (+ pyruvate + 4.5 g/l glucose + glutamate) serum free for 24 hr.

-Transwell co-culture experiments

MuSCs and FAP cells were co-cultured by using inserts with 1.0 μm porous membrane to avoid direct contact between populations.

Cell culture inserts with 1.0-um pore (#353102, #353104, Falcon) and 6 or 24 -well culture plates (BD Bioscience) were used for transwell co-culture. Freshly sorted MuSCs were plated in the bottom of the plate, while FAP cells were plated on the upper insert.

6.6 Single fibers isolation

Single fibers were isolated using Pasut (2013) and Moyle's protocol (2014) from tibialis anterior, extensor digitorum longus, gastrocnemius and soleus muscles of C57BL6J-WT mice and cultured in proliferating medium (GM1: DMEM + pyruvate +4.5 g/l glucose + glutamate, 10% horse serum (HS), 0.5% Chicken Embryo Extract) for 24 hours, then exposed for the next 24 hrs to GM1 conditioned media derived from culture of FAPs (MEDIA-FAPs) isolated from young mdx mouse treated for 15 days with vehicle (CTR) or mdx mice treated with TSA (TSA) or media isolated from FAPs CTR and TSA pre-treated with the GW4869 to inhibit exosome biogenesis. In a parallel, independent experiment, single fibers were exposed to exosomes (EXO-FAPs) purified from MEDIA-FAPs and added to GM1 for 24 hours.

6.7 Cell treatments

The transfection of FAPs with pCT-CD63-GFP plasmid (#CYTO120-PA-1, System Biosciences) and with a GFP-control vector (mock) in cell culture inserts was accomplished

using Lipofectamine 2000 (#12566014, Thermofisher Scientific) 6 hours before MuSCs co-colture. Transwell co-cultures were maintained in GM2 medium for 24hrs and then harvested for GFP-analyses.
To decrease FAP-exosomes release, GW4869 (10 uM, #D1692, Sigma) was added to FAPs culture 30' before the co-colture setting with MuSCs. To wash away any residual trace of GW4869, FAPs media was refreshed right before co-culture.
For AntagomiR FAPs isolated from mdx mice TSA treated, were transfected with AntagomiR-206 (mmu-miR-206-3p miRCURY LNA™ microRNA inhibitor, Exiqon) and mock (miRCURY LNA™ microRNA inhibitor control #199006, Exiqon) using Dharmafect3.0 (#T2003-03, Thermo Fisher Scientific) according to manufacturer instructions; after 6 hours the medium was replaced with DMEM serum free for 24 hours before exosome isolation and purification.
For Drosha SiRNA treatments, *in vivo* TSA treated FAPs on transwell were transfected with commercially available Drosha siRNA using Dharmafect3.0 (Dharmacon) according to manufacturer instructions; after 6 hours FAPs were put in co-culture with MuSCs.
To stain FAPs derived exosomes, FAP cells were incubated with the lipidic dye PKH-67 (#P7333, Sigma) according to manufacturer instructions prior to transwell co-culture with MuSCs.
In ex-vivo experiments FAP-derived Exosomes (10ug) isolated by TEIR were put in culture with MuSCs or with myofibers in the cell culture media.

6.8 Immunofluorescence

For immunofluorescence analysis, cryo-sections and cells were fixed in 4% PFA for 10 min and permeabilized with 100% cold acetone (#32201, Sigma) for 6 min at -20°C or 100% cold Methanol (#32213, Sigma) for 6 min at -20° or with 0,25%

Triton for 15 min at RT. Muscle sections were blocked for 1h with a solution containing 4% BSA (#A7030, Sigma) in PBS. The primary antibodies incubation were performed O.N. at 4°C and then the antibody binding specificity was revealed using secondary antibodies coupled to Alexa Fluor 488, 594, or 647 (Invitrogen). Sections were incubated with DAPI in PBS for 5 minutes for nuclear staining, washed in PBS, and mounted with glycerol 3:1 in PBS. The primary antibodies used for immunofluorescences are: rabbit anti-Laminin (1/400, #L9393, Sigma); rat anti-SCA1 (1/100, #11-5981-82 Ly-6A/E FITC, eBioscience,); mouse anti-eMyHC (1/20, #F1.652, Developmental Studies Hybridoma Bank, DSHB, http://dshb.biology.uiowa.edu/F1-652); mouse anti-MF20 (1:20, Developmental Studies Hybridoma Bank, DSHB, http://dshb.biology.uiowa.edu/MF-20), mouse anti-PAX7 (1/10, Developmental Studies Hybridoma Bank, DSHB, http://dshb.biology.uiowa.edu/PAX7), rabbit anti-MyoD-318 (#SC760, Santa Cruz Biotechnology), EDU (#C10350, Invitrogen), rat anti-CD63 PE (#143904, clone NUG-2, Biolegend) and Myeloperoxidase/MPO (1/100 #MAB3174, R&D).

6.9 Exosomes Isolation

Exosomes were isolated from FAPs serum free cell culture medium in parallel with Total exosomes isolation reagent - TEIR- (#4478359, Invitrogen by Thermo Fisher Scientific) according to manufacturer instructions and with previously published ultracentrifugation method -UC- (Thery et al., 2006). The ultracentrifugation isolation method included a penultimate centrifugation step (10,000 x g for 30 min) that allowed the removal/isolation of larger microvesicles for the subsequent pelleting of nanovesicles, comprised mainly of exosomes. The pellet of exosomes isolated in both methods was resuspended in PBS for biophysics and molecular analyses.

Exosomes were purified from tibialis anterior cut into small pieces in serum-free DMEM (24 h). Cell debris and organelles were eliminated by centrifugation at 2,000g for 20 min and exosomes were isolated using TEIR.

6.10 Exosome characterization

Exosome size distribution was determined by Dynamic Light Scattering (DLS) measurements. Collected exosome samples were diluted to a final concentration of 15 □g/ml total protein content in order to avoid multiple scattering artifacts. Static and dynamic light scattering measurements were performed at 20^0C by using a Brookhaven Instruments BI-9000 correlator and a solid-state laser tuned at 532 nm. Scattered intensity autocorrelation functions g2(t) have been analyzed by using multiple gamma functions for the diffusion coefficient and therefore by using the classic Stokes-Einstein relation to determine the size distribution P(D) of vesicles, where the size parameter D is actually the hydrodynamic radius of diffusing vesicles (Noto et al.2012).
Exosome morphology was examined *for* Scanning electron microscopy analysis.
Exosomes isolated and purified from FAPs by TEIR were fixed in 4% (v/v) paraformaldehyde, dehydrated by a series of incubations in 30%, 50%, and 70% (v/v) ethanol and dried on aluminium support for SEM. Exosomes isolated were coated with gold. A SEM LEO 1450VP (Carl Zeiss Meditec, Oberkochen, Germany) was employed to acquire backscattered electron images using 20 keV electrons leading to an information depth of about 1.5 μm. Images with a scan size of 30 × 30 μm were acquired, at a resolution of 1024 × 1024 pixels (Carpentieri et al., 2016).

6.11 Exosome labeling

Acridine Orange
To detect nucleic acid content, FAPs derived exosomes (10μg) isolated by TEIR, were labeled with acridine orange -AO- (#235474, Sigma) (100 mg/ml) for 30 minutes at room temperature and added to MuSCs in order to reveal by immunofluorescence the RNA exchanged from FAPs to MuSCs.

PKH-67
To visualize exosomes, FAPs-derived Exosomes (10μg) are stained for 5 minutes at room temperature RT with 0.5μl of PKH67 Green Fluorescent Cell Linker Kit for General Cell Membrane Labeling (#P7333, Sigma) and then polished with the exosome spin columns (#4484449, Invitrogen by Thermo Fisher Scientific) following the manufacturer protocol. The stained exosomes are detected by immunofluorescence into myo-fibers and by cyto-fluorimetric analysis in mice muscle after their *in-vivo* injection.

6.12 Exosomal content

Protein
Exosomes isolated were lysed for protein extraction in RIPA buffer (50 mM Tris-HCl, pH 7.4; 150 mM NaCl; 1% NP-40; protease inhibitors). The total exosomal protein content was quantified using the micro bicinchoninic acid protein assay (BCA) (#23235, Thermo Fisher scientific).
Western blot
Western blot was performed using antibodies against the following proteins: rabbit anti-CD63 (1/300, H-193, Santa Cruz Biotechnology), mouse anti-Hsp70 (1/2500, clone BRM-22,

Sigma-Aldrich), rabbit anti-Calnexin (1/1000, NB100-1965, Novus Biologicals), rabbit anti-Flotillin-1 (1/200, H-104, Santa Cruz Biotechnology).
As total lysate normalization we used Ponceau quantifiction.

microRNA
Total exosomal RNA was extracted with Total Exosome RNA Protein Isolation Kit (#4478545, Thermo Fisher Scientific). TaqMan MicroRNA Assays were performed according to the manufacturer's recommended protocols (Applied Biosystems) The threshold cycle (Ct) were defined as the fractional cycle number at which the fluorescence passes the fixed threshold. U6 snRNA served as an endogenous control for normalization.
In particular, total exosomal-RNA was retro-transcribed using TaqMan MicroRNA Reverse Transcription Kit (#4366596, ThermoFisher Scientific)
For greater sensitivity, the cDNA was pre-amplified using Taqman PREAMP master mix (#4391128, ThermoFisher Scientific) and Megaplex PreAMp Primers and then amplified using high multiplexed Megaplex Primer Pool (#4444766, ThermoFisher Scientific) and the TaqMan 2X Universal Master Mix II (#4440040, ThermoFisher Scientific) on TaqMan rodent MicroRNA A/B cards Array version 3.0 (#4444909, ThermoFisher Scientific).
qRT–PCR
For miRs validation, Total exosomal RNA was extracted with Total Exosome RNA Protein Isolation Kit (#4478545, Invitrogen by Thermo Fisher Scientific) and was retro-transcribed using the Qiagen reverse transcription kit (miScript II RT Kit, #218161, Qiagen) and pre-amplified using (miScript PreAMP PCR Kit, # 331451, Qiagen).
Real-time qPCR was performed using (miScript SYBR Green PCR Kit, #218073, Qiagen) and using primers reported in table (KRT). All the conditions are provided in the manufacturer protocol.

6.13 FAPs derived Exosome intra-muscular injection

FAPs-derived exosomes at a final concentration of 10µg in 20µL of PBS1x (0.5µg/µl) were injected 3 times in left Tibialis

Anterior (TA) of C57BL6/mdx mice: every 7 days for 21 days. The right TA was injected with vehicle (20 µL PBS1x) following the same timing described for exosomes injection.

6.14 RNA-sequencing

For RNA-sequencing sample preparation, MuSCs and FAPs were freshly isolated by FACS from 6 C57Bl6 mdx male mice 8-weeks old treated or not with TSA for 15 days. RNA was collected using Trizol**)** reagent (#T9424, Sigma**)**. About 100 ng/µL of total RNA was sent in duplicate to IGA (Istituto di Genomica Applicata, Udine) for RNA sequencing using Illumina TruSeq Stranded Total RNA kit Ribo-Zero GOLD on Illumina Hiseq2500 platform.

6. 15 Quantification and statistical analysis

The number of independent experimental replications and precision measures are reported in the figure legends (n, mean ± sem or n, mean ± sd). Statistical analyses were performed using the Microsoft office excell 2016 statistical utilities. Statistical significance was assessed by the two-tailed Student's t test. P-value < 0.05 was considered as statistically significant.

6.16 Data and Software availability

The cells positive for the stainings described in the text were quantified using ImageJ software (https://imagej.nih.gov/ij/download.html). The cross-sectional area (CSA), was also calculated using the ImageJ software and Macro seg 5 modif.ijm specific plugin. Fibrotic areas were measured from sections evaluating image analysis algorithms for colour deconvolution. ImageJ was used for image processing, the original image was segmented with three clusters and the plugin assumes images generated by color subtraction (white representing background, blue collagen, and magenta non collagen regions).
FACS profile analysis of MuSCs and FAPs were performed using Flowjo software (https://www.flowjo.com).
The RNA sequencing analysis was performed Mapping more than 20 millions of reads for each sample to the Mus Musculus GRCm38.78 genome using TopHat 2.0.9. Read count was performed with HTSeq-0.6.1p1. Mapped reads were analysed with R-studio using DESeq2 to obtain normalized RPKM, P-Value, P-adjusted and log2fold changes values. Genes were considered differentially expressed if the P-adjusted value was <0.1.
MiR pathway analysis was performed using miRPath based on predicted miR targets provided by the DIANA-microT-CDS algorithm and/or experimentally validated miR interactions derived from DIANA-TarBase v6.0 (http://www.microrna.gr/miRPathv2).

6.17 Prediction of miR-mRNA interactions and network construction.

Data from RNAseq (padj<0.1) in MuSCs (treated or not with TSA) and Microarray analysis in FAPs (treated or not with TSA) derived exosomes, were uploaded in IPA

(https://www.qiagenbioinformatics.com/products/ingenuity-pathway-analysis/). With the IPA tool "miR Target Filter" the miR upregulated in FAPs exosomes were intersected with transcripts down-regulated in MuSCs after TSA treatment. Only interactions experimentally observed and highly predicted were selected for downstream analysis. Notch pathway was extrapolated from IPA database using the tool "grow", while its modulation was predicted by the Molecular Activity Predictor (MAP) tool. The cartoon was realized with IPA path-designer

OLIGOS TABLE

MS00033740	Qiagen	Hs_RNU6-2_1
MS00001372	Qiagen	Mm_miR-29a_1
MS00033761	Qiagen	Mm_miR-494_2
MS00011704	Qiagen	Mm_miR-30a_1
MS00002387	Qiagen	Mm_miR-449_1
MS00001869	Qiagen	Mm_miR-206_1

7. References

Amirouche, A., Tadesse, H., Miura, P., Bélanger, G., Lunde, J.A., Côté, J., and Jasmin, B.J. (2014). Converging pathways involving microRNA-206 and the RNA-binding protein KSRP control post-transcriptionally utrophin A expression in skeletal muscle. Nucleic Acids Res. *42*, 3982–3997.

Asakura, A., Seale, P., Girgis-Gabardo, A., and Rudnicki, M.A. (2002). Myogenic specification of side population cells in skeletal muscle. J. Cell Biol. *159*, 123–134.

Baietti, M.F., Zhang, Z., Mortier, E., Melchior, A., Degeest, G., Geeraerts, A., Ivarsson, Y., Depoortere, F., Coomans, C., Vermeiren, E., et al. (2012). Syndecan-syntenin-ALIX regulates the biogenesis of exosomes. Nat. Cell Biol. *14*, 677–685.

Bartel, D.P. (2004). MicroRNAs: genomics, biogenesis, mechanism, and function. Cell *116*, 281–297.

Basu, J., and Ludlow, J.W. (2016). Exosomes for repair, regeneration and rejuvenation. Expert Opin. Biol. Ther. *16*, 489–506.

Beauchamp, J.R., Heslop, L., Yu, D.S.W., Tajbakhsh, S., Kelly, R.G., Wernig, A., Buckingham, M.E., Partridge, T.A., and Zammit, P.S. (2000). Expression of Cd34 and Myf5 Defines the Majority of Quiescent Adult Skeletal Muscle Satellite Cells. J. Cell Biol. *151*, 1221–1234.

Bettica, P., Petrini, S., D'Oria, V., D'Amico, A., Catteruccia, M., Pane, M., Sivo, S., Magri, F., Brajkovic, S., Messina, S., et al. (2016). Histological effects of givinostat in boys with Duchenne muscular dystrophy. Neuromuscul. Disord. NMD *26*, 643–649.

Bischoff, R. (1986). Proliferation of muscle satellite cells on intact myofibers in culture. Dev. Biol. *115*, 129–139.

Bober, E., Franz, T., Arnold, H.H., Gruss, P., and Tremblay, P. (1994). Pax-3 is required for the development of limb muscles: a possible role for the migration of dermomyotomal muscle progenitor cells. Dev. Camb. Engl. *120*, 603–612.

Booth, A.M., Fang, Y., Fallon, J.K., Yang, J.-M., Hildreth, J.E.K., and Gould, S.J. (2006). Exosomes and HIV Gag bud from endosome-like domains of the T cell plasma membrane. J. Cell Biol. *172*, 923–935.

Borges, F.T., Melo, S.A., Özdemir, B.C., Kato, N., Revuelta, I., Miller, C.A., Gattone, V.H., LeBleu, V.S., and Kalluri, R. (2013). TGF-β1-containing exosomes from injured epithelial cells activate fibroblasts to initiate tissue regenerative responses and fibrosis. J. Am. Soc. Nephrol. JASN *24*, 385–392.

Boutz, P.L., Chawla, G., Stoilov, P., and Black, D.L. (2007). MicroRNAs regulate the expression of the alternative splicing factor nPTB during muscle development. Genes Dev. *21*, 71–84.

Braicu, C., Tomuleasa, C., Monroig, P., Cucuianu, A., Berindan-Neagoe, I., and Calin, G.A. (2015). Exosomes as divine messengers: are they the Hermes of modern molecular oncology? Cell Death Differ. *22*, 34–45.

Cacchiarelli, D., Martone, J., Girardi, E., Cesana, M., Incitti, T., Morlando, M., Nicoletti, C., Santini, T., Sthandier, O., Barberi, L., et al. (2010). MicroRNAs involved in molecular circuitries relevant for the Duchenne muscular dystrophy pathogenesis are controlled by the dystrophin/nNOS pathway. Cell Metab. *12*, 341–351.

Cacchiarelli, D., Legnini, I., Martone, J., Cazzella, V., D'Amico, A., Bertini, E., and Bozzoni, I. (2011). miRNAs as serum biomarkers for Duchenne muscular dystrophy. EMBO Mol. Med. *3*, 258–265.

Caretti, G., Di Padova, M., Micales, B., Lyons, G.E., and Sartorelli, V. (2004). The Polycomb Ezh2 methyltransferase regulates muscle gene expression and skeletal muscle differentiation. Genes Dev. *18*, 2627–2638.

Carpentieri, A., Cozzoli, E., Scimeca, M., Bonanno, E., Sardanelli, A.M., and Gambacurta, A. (2016). Differentiation of human neuroblastoma cells toward the osteogenic lineage by mTOR inhibitor. Cell Death Dis. *7*, e2202.

Chang, N.C., Chevalier, F.P., and Rudnicki, M.A. (2016). Satellite Cells in Muscular Dystrophy - Lost in Polarity. Trends Mol. Med. *22*, 479–496.

Chaput, N., and Théry, C. (2011). Exosomes: immune properties and potential clinical implementations. Semin. Immunopathol. *33*, 419–440.

Chargé, S.B.P., and Rudnicki, M.A. (2004). Cellular and Molecular Regulation of Muscle Regeneration. Physiol. Rev. *84*, 209–238.

Chen, J.-F., Mandel, E.M., Thomson, J.M., Wu, Q., Callis, T.E., Hammond, S.M., Conlon, F.L., and Wang, D.-Z. (2006). The role of microRNA-1 and microRNA-133 in skeletal muscle proliferation and differentiation. Nat. Genet. *38*, 228–233.

Chen, J.-F., Tao, Y., Li, J., Deng, Z., Yan, Z., Xiao, X., and Wang, D.-Z. (2010). microRNA-1 and microRNA-206 regulate skeletal muscle satellite cell proliferation and differentiation by repressing Pax7. J. Cell Biol. *190*, 867–879.

Choi, J.S., Yoon, H.I., Lee, K.S., Choi, Y.C., Yang, S.H., Kim, I.-S., and Cho, Y.W. (2016). Exosomes from differentiating human skeletal muscle cells trigger myogenesis of stem cells and provide biochemical cues for skeletal muscle regeneration. J. Control. Release Off. J. Control. Release Soc. *222*, 107–115.

Collino, F., Deregibus, M.C., Bruno, S., Sterpone, L., Aghemo, G., Viltono, L., Tetta, C., and Camussi, G. (2010). Microvesicles derived from adult human bone marrow and tissue specific mesenchymal stem cells shuttle selected pattern of miRNAs. PloS One *5*, e11803.

Colombo, M., Moita, C., van Niel, G., Kowal, J., Vigneron, J., Benaroch, P., Manel, N., Moita, L.F., Théry, C., and Raposo, G. (2013). Analysis of ESCRT functions in exosome biogenesis, composition and secretion highlights the heterogeneity of extracellular vesicles. J. Cell Sci. *126*, 5553–5565.

Colussi, C., Mozzetta, C., Gurtner, A., Illi, B., Rosati, J., Straino, S., Ragone, G., Pescatori, M., Zaccagnini, G., Antonini, A., et al. (2008). HDAC2 blockade by nitric oxide and histone deacetylase inhibitors reveals a common target in Duchenne muscular dystrophy treatment. Proc. Natl. Acad. Sci. U. S. A. *105*, 19183–19187.

Consalvi, S., Saccone, V., Giordani, L., Minetti, G., Mozzetta, C., and Puri, P.L. (2011). Histone deacetylase inhibitors in the treatment of muscular dystrophies: epigenetic drugs for genetic diseases. Mol. Med. Camb. Mass *17*, 457–465.

Consalvi, S., Mozzetta, C., Bettica, P., Germani, M., Fiorentini, F., Del Bene, F., Rocchetti, M., Leoni, F., Monzani, V., Mascagni, P., et al. (2013). Preclinical studies in the mdx mouse model of duchenne muscular dystrophy with the histone deacetylase inhibitor givinostat. Mol. Med. Camb. Mass *19*, 79–87.

Consalvi, S., Saccone, V., and Mozzetta, C. (2014). Histone deacetylase inhibitors: a potential epigenetic treatment for Duchenne muscular dystrophy. Epigenomics *6*, 547–560.

Crist, C.G., Montarras, D., Pallafacchina, G., Rocancourt, D., Cumano, A., Conway, S.J., and Buckingham, M. (2009). Muscle stem cell behavior is modified by microRNA-27 regulation of Pax3 expression. Proc. Natl. Acad. Sci. U. S. A. *106*, 13383–13387.

De Luca, A. (2012). Pre-clinical drug tests in the mdx mouse as a model of dystrophinopathies: an overview. Acta Myol. Myopathies Cardiomyopathies Off. J. Mediterr. Soc. Myol. *31*, 40–47.

Dellavalle, A., Maroli, G., Covarello, D., Azzoni, E., Innocenzi, A., Perani, L., Antonini, S., Sambasivan, R., Brunelli, S., Tajbakhsh, S., et al. (2011). Pericytes resident in postnatal skeletal muscle differentiate into muscle fibres and generate satellite cells. Nat. Commun. *2*, 499.

Dey, B.K., Gagan, J., and Dutta, A. (2011). miR-206 and -486 induce myoblast differentiation by downregulating Pax7. Mol. Cell. Biol. *31*, 203–214.

Dumont, N.A., Wang, Y.X., von Maltzahn, J., Pasut, A., Bentzinger, C.F., Brun, C.E., and Rudnicki, M.A. (2015). Dystrophin expression in muscle stem cells regulates their polarity and asymmetric division. Nat. Med. *21*, 1455–1463.

EL Andaloussi, S., Mäger, I., Breakefield, X.O., and Wood, M.J.A. (2013). Extracellular vesicles: biology and emerging therapeutic opportunities. Nat. Rev. Drug Discov. *12*, 347–357.

Elia, L., Contu, R., Quintavalle, M., Varrone, F., Chimenti, C., Russo, M.A., Cimino, V., De Marinis, L., Frustaci, A., Catalucci, D., et al. (2009). Reciprocal regulation of microRNA-1 and insulin-like growth factor-1 signal transduction cascade in cardiac and skeletal muscle in physiological and pathological conditions. Circulation *120*, 2377–2385.

Fang, Y., Wu, N., Gan, X., Yan, W., Morrell, J.C., and Gould, S.J. (2007). Higher-order oligomerization targets plasma membrane proteins and HIV gag to exosomes. PLoS Biol. *5*, e158.

Filipowicz, W., Bhattacharyya, S.N., and Sonenberg, N. (2008). Mechanisms of post-transcriptional regulation by microRNAs: are the answers in sight? Nat. Rev. Genet. *9*, 102–114.

Fischle, W., Wang, Y., and Allis, C.D. (2003). Histone and chromatin cross-talk. Curr. Opin. Cell Biol. *15*, 172–183.

Forterre, A., Jalabert, A., Chikh, K., Pesenti, S., Euthine, V., Granjon, A., Errazuriz, E., Lefai, E., Vidal, H., and Rome, S. (2014). Myotube-derived exosomal miRNAs downregulate Sirtuin1 in myoblasts during muscle cell differentiation. Cell Cycle Georget. Tex *13*, 78–89.

Frontera, W.R., and Ochala, J. (2015). Skeletal Muscle: A Brief Review of Structure and Function. Calcif. Tissue Int. *96*, 183–195.

Fry, C.S., Kirby, T.J., Kosmac, K., McCarthy, J.J., and Peterson, C.A. (2017). Myogenic Progenitor Cells Control Extracellular Matrix Production by Fibroblasts during Skeletal Muscle Hypertrophy. Cell Stem Cell *20*, 56–69.

Gagan, J., Dey, B.K., Layer, R., Yan, Z., and Dutta, A. (2012). Notch3 and Mef2c proteins are mutually antagonistic via Mkp1 protein and miR-1/206 microRNAs in differentiating myoblasts. J. Biol. Chem. *287*, 40360–40370.

Goljanek-Whysall, K., Sweetman, D., and Münsterberg, A.E. (2012). microRNAs in skeletal muscle differentiation and disease. Clin. Sci. *123*, 611–625.

Greco, S., De Simone, M., Colussi, C., Zaccagnini, G., Fasanaro, P., Pescatori, M., Cardani, R., Perbellini, R., Isaia, E., Sale, P., et al. (2009). Common micro-RNA signature in skeletal muscle damage and regeneration induced by Duchenne muscular dystrophy and acute ischemia. FASEB J. Off. Publ. Fed. Am. Soc. Exp. Biol. *23*, 3335–3346.

Guasconi, V., and Puri, P.L. (2009). Chromatin: the interface between extrinsic cues and the epigenetic regulation of muscle regeneration. Trends Cell Biol. *19*, 286–294.

Guescini, M., Genedani, S., Stocchi, V., and Agnati, L.F. (2010). Astrocytes and Glioblastoma cells release exosomes carrying mtDNA. J. Neural Transm. Vienna Austria 1996 *117*, 1–4.

Guess, M.G., Barthel, K.K.B., Harrison, B.C., and Leinwand, L.A. (2015). miR-30 family microRNAs regulate myogenic differentiation and provide negative feedback on the microRNA pathway. PloS One *10*, e0118229.

Harding, C., Heuser, J., and Stahl, P. (1984). Endocytosis and intracellular processing of transferrin and colloidal gold-transferrin in rat reticulocytes: demonstration of a pathway for receptor shedding. Eur. J. Cell Biol. *35*, 256–263.

He, W.A., Calore, F., Londhe, P., Canella, A., Guttridge, D.C., and Croce, C.M. (2014). Microvesicles containing miRNAs promote muscle cell death in cancer cachexia via TLR7. Proc. Natl. Acad. Sci. U. S. A. *111*, 4525–4529.

Henne, W.M., Stenmark, H., and Emr, S.D. (2013). Molecular mechanisms of the membrane sculpting ESCRT pathway. Cold Spring Harb. Perspect. Biol. *5*.

Heredia, J.E., Mukundan, L., Chen, F.M., Mueller, A.A., Deo, R.C., Locksley, R.M., Rando, T.A., and Chawla, A. (2013). Type 2 innate signals stimulate fibro/adipogenic progenitors to facilitate muscle regeneration. Cell *153*, 376–388.

Hirai, H., Verma, M., Watanabe, S., Tastad, C., Asakura, Y., and Asakura, A. (2010). MyoD regulates apoptosis of myoblasts through microRNA-mediated down-regulation of Pax3. J. Cell Biol. *191*, 347–365.

Hoffman, E.P., and Dressman, D. (2001). Molecular pathophysiology and targeted therapeutics for muscular dystrophy. Trends Pharmacol. Sci. *22*, 465–470.

Hunter, M.P., Ismail, N., Zhang, X., Aguda, B.D., Lee, E.J., Yu, L., Xiao, T., Schafer, J., Lee, M.-L.T., Schmittgen, T.D., et al. (2008). Detection of microRNA expression in human peripheral blood microvesicles. PloS One *3*, e3694.

Iraci, N., Leonardi, T., Gessler, F., Vega, B., and Pluchino, S. (2016). Focus on Extracellular Vesicles: Physiological Role and Signalling Properties of Extracellular Membrane Vesicles. Int. J. Mol. Sci. *17*, 171.

Joe, A.W.B., Yi, L., Natarajan, A., Le Grand, F., So, L., Wang, J., Rudnicki, M.A., and Rossi, F.M.V. (2010). Muscle injury activates resident fibro/adipogenic progenitors that facilitate myogenesis. Nat. Cell Biol. *12*, 153–163.

Juan, A.H., Kumar, R.M., Marx, J.G., Young, R.A., and Sartorelli, V. (2009). Mir-214-dependent regulation of the polycomb protein Ezh2 in skeletal muscle and embryonic stem cells. Mol. Cell *36*, 61–74.

Katzmann, D.J., Babst, M., and Emr, S.D. (2001). Ubiquitin-dependent sorting into the multivesicular body pathway requires the function of a conserved endosomal protein sorting complex, ESCRT-I. Cell *106*, 145–155.

Kim, H.K., Lee, Y.S., Sivaprasad, U., Malhotra, A., and Dutta, A. (2006). Muscle-specific microRNA miR-206 promotes muscle differentiation. J. Cell Biol. *174*, 677–687.

Kim, V.N., Han, J., and Siomi, M.C. (2009). Biogenesis of small RNAs in animals. Nat. Rev. Mol. Cell Biol. *10*, 126–139.
Kitamoto, T., and Hanaoka, K. (2010). Notch3 null mutation in mice causes muscle hyperplasia by repetitive muscle regeneration. Stem Cells Dayt. Ohio *28*, 2205–2216.

Kosaka, N., Iguchi, H., Yoshioka, Y., Takeshita, F., Matsuki, Y., and Ochiya, T. (2010). Secretory mechanisms and intercellular transfer of microRNAs in living cells. J. Biol. Chem. *285*, 17442–17452.

Kowal, J., Tkach, M., and Théry, C. (2014). Biogenesis and secretion of exosomes. Curr. Opin. Cell Biol. *29*, 116–125.

Le Grand, F., and Rudnicki, M.A. (2007). Skeletal muscle satellite cells and adult myogenesis. Curr. Opin. Cell Biol. *19*, 628–633.

Lee, Y., El Andaloussi, S., and Wood, M.J.A. (2012). Exosomes and microvesicles: extracellular vesicles for genetic information transfer and gene therapy. Hum. Mol. Genet. *21*, R125-134.

Lemos, D.R., Babaeijandaghi, F., Low, M., Chang, C.-K., Lee, S.T., Fiore, D., Zhang, R.-H., Natarajan, A., Nedospasov, S.A., and Rossi, F.M.V. (2015). Nilotinib reduces muscle fibrosis in chronic muscle injury by promoting TNF-mediated apoptosis of fibro/adipogenic progenitors. Nat. Med. *21*, 786–794.

Lenassi, M., Cagney, G., Liao, M., Vaupotic, T., Bartholomeeusen, K., Cheng, Y., Krogan, N.J., Plemenitas, A., and Peterlin, B.M. (2010). HIV Nef is secreted in exosomes and triggers apoptosis in bystander CD4+ T cells. Traffic Cph. Den. *11*, 110–122.

Liu, N., Williams, A.H., Maxeiner, J.M., Bezprozvannaya, S., Shelton, J.M., Richardson, J.A., Bassel-Duby, R., and Olson, E.N. (2012). microRNA-206 promotes skeletal muscle regeneration and delays progression of Duchenne muscular dystrophy in mice. J. Clin. Invest. *122*, 2054–2065.

Lorenzo, G., and Puri, P.L. (2013). Epigenetic control of skeletal muscle regeneration: integrating genetic determinants and environmental changes. FEBS J. *280*, 4014–4025.

Lötvall, J., Hill, A.F., Hochberg, F., Buzás, E.I., Di Vizio, D., Gardiner, C., Gho, Y.S., Kurochkin, I.V., Mathivanan, S., Quesenberry, P., et al. (2014). Minimal experimental requirements for definition of extracellular vesicles and their functions: a position statement from the International Society for Extracellular Vesicles. J. Extracell. Vesicles *3*, 26913.

Ma, G., Wang, Y., Li, Y., Cui, L., Zhao, Y., Zhao, B., and Li, K. (2015). MiR-206, a Key Modulator of Skeletal Muscle Development and Disease. Int. J. Biol. Sci. *11*, 345–352.

Mal, A., Sturniolo, M., Schiltz, R.L., Ghosh, M.K., and Harter, M.L. (2001). A role for histone deacetylase HDAC1 in modulating the transcriptional activity of MyoD: inhibition of the myogenic program. EMBO J. *20*, 1739–1753.

Manzur, A.Y., Kinali, M., and Muntoni, F. (2008). Update on the management of Duchenne muscular dystrophy. Arch. Dis. Child. *93*, 986–990.

Marsh, M., and van Meer, G. (2008). Cell biology. No ESCRTs for exosomes. Science *319*, 1191–1192.

Mauro, A. (1961). SATELLITE CELL OF SKELETAL MUSCLE FIBERS. J. Biophys. Biochem. Cytol. *9*, 493–495.

McCarthy, J.J. (2011). The MyomiR Network in Skeletal Muscle Plasticity. Exerc. Sport Sci. Rev. *39*, 150–154.

McKinsey, T.A., Zhang, C.L., Lu, J., and Olson, E.N. (2000). Signal-dependent nuclear export of a histone deacetylase regulates muscle differentiation. Nature *408*, 106–111.

Michelet, X., Djeddi, A., and Legouis, R. (2010). Developmental and cellular functions of the ESCRT machinery in pluricellular organisms. Biol. Cell *102*, 191–202.

Minetti, G.C., Colussi, C., Adami, R., Serra, C., Mozzetta, C., Parente, V., Fortuni, S., Straino, S., Sampaolesi, M., Di Padova, M., et al. (2006). Functional and morphological recovery of dystrophic muscles in mice treated with deacetylase inhibitors. Nat. Med. *12*, 1147–1150.

Mitchell, K.J., Pannérec, A., Cadot, B., Parlakian, A., Besson, V., Gomes, E.R., Marazzi, G., and Sassoon, D.A. (2010). Identification and characterization of a non-satellite cell muscle resident progenitor during postnatal development. Nat. Cell Biol. *12*, 257–266.

Montecalvo, A., Larregina, A.T., Shufesky, W.J., Stolz, D.B., Sullivan, M.L.G., Karlsson, J.M., Baty, C.J., Gibson, G.A., Erdos, G., Wang, Z., et al. (2012). Mechanism of transfer of functional microRNAs between mouse dendritic cells via exosomes. Blood *119*, 756–766.

Mozzetta, C., Minetti, G., and Puri, P.L. (2009). Regenerative pharmacology in the treatment of genetic diseases: The paradigm of muscular dystrophy. Int. J. Biochem. Cell Biol. *41*, 701–710.

Mozzetta, C., Consalvi, S., Saccone, V., Tierney, M., Diamantini, A., Mitchell, K.J., Marazzi, G., Borsellino, G., Battistini, L., Sassoon, D., et al. (2013). Fibroadipogenic progenitors mediate the ability of HDAC inhibitors to promote regeneration in dystrophic muscles of young, but not old Mdx mice. EMBO Mol. Med. *5*, 626–639.

Muñoz-Cánoves, P., and Serrano, A.L. (2015). Macrophages decide between regeneration and fibrosis in muscle. Trends Endocrinol. Metab. *26*, 449–450.

Muntoni, F., Torelli, S., and Ferlini, A. (2003). Dystrophin and mutations: one gene, several proteins, multiple phenotypes. Lancet Neurol. *2*, 731–740.

Musarò, A. (2014). The Basis of Muscle Regeneration.
Mutsaers, S.E., Bishop, J.E., McGrouther, G., and Laurent, G.J. (1997). Mechanisms of tissue repair: from wound healing to fibrosis. Int. J. Biochem. Cell Biol. *29*, 5–17.

Nakamura, Y., Miyaki, S., Ishitobi, H., Matsuyama, S., Nakasa, T., Kamei, N., Akimoto, T., Higashi, Y., and Ochi, M. (2015). Mesenchymal-stem-cell-derived exosomes accelerate skeletal muscle regeneration. FEBS Lett. *589*, 1257–1265.

Olguin, H.C., and Olwin, B.B. (2004). Pax-7 up-regulation inhibits myogenesis and cell cycle progression in satellite cells: a potential mechanism for self-renewal. Dev. Biol. *275*, 375–388.

Pan, B.T., and Johnstone, R.M. (1983). Fate of the transferrin receptor during maturation of sheep reticulocytes in vitro: selective externalization of the receptor. Cell *33*, 967–978.

Puri, P.L., Iezzi, S., Stiegler, P., Chen, T.T., Schiltz, R.L., Muscat, G.E., Giordano, A., Kedes, L., Wang, J.Y., and Sartorelli, V. (2001). Class I histone deacetylases sequentially interact with MyoD and pRb during skeletal myogenesis. Mol. Cell *8*, 885–897.

Rao, P.K., Kumar, R.M., Farkhondeh, M., Baskerville, S., and Lodish, H.F. (2006). Myogenic factors that regulate expression of muscle-specific microRNAs. Proc. Natl. Acad. Sci. U. S. A. *103*, 8721–8726.

Raposo, G., and Stoorvogel, W. (2013). Extracellular vesicles: Exosomes, microvesicles, and friends. J Cell Biol *200*, 373–383.

Raposo, G., Nijman, H.W., Stoorvogel, W., Liejendekker, R., Harding, C.V., Melief, C.J., and Geuze, H.J. (1996). B lymphocytes secrete antigen-presenting vesicles. J. Exp. Med. *183*, 1161–1172.

Ratajczak, M.Z., Kucia, M., Jadczyk, T., Greco, N.J., Wojakowski, W., Tendera, M., and Ratajczak, J. (2012). Pivotal role of paracrine effects in stem cell therapies in regenerative medicine: can we translate stem cell-secreted paracrine factors and microvesicles into better therapeutic strategies? Leukemia *26*, 1166–1173.

Romancino, D.P., Paterniti, G., Campos, Y., De Luca, A., Di Felice, V., d'Azzo, A., and Bongiovanni, A. (2013). Identification and characterization of the nano-sized vesicles released by muscle cells. FEBS Lett. *587*, 1379–1384.

Rosenberg, M.I., Georges, S.A., Asawachaicharn, A., Analau, E., and Tapscott, S.J. (2006). MyoD inhibits Fstl1 and Utrn expression by inducing transcription of miR-206. J. Cell Biol. *175*, 77–85.

Rudnicki, M.A., Schnegelsberg, P.N., Stead, R.H., Braun, T., Arnold, H.H., and Jaenisch, R. (1993). MyoD or Myf-5 is required for the formation of skeletal muscle. Cell *75*, 1351–1359.

Saccone, V., and Puri, P.L. (2010). Epigenetic regulation of skeletal myogenesis. Organogenesis *6*, 48–53.

Saccone, V., Consalvi, S., Giordani, L., Mozzetta, C., Barozzi, I., Sandoná, M., Ryan, T., Rojas-Muñoz, A., Madaro, L., Fasanaro, P., et al. (2014). HDAC-regulated myomiRs control BAF60 variant exchange and direct the functional phenotype of fibro-adipogenic progenitors in dystrophic muscles. Genes Dev. *28*, 841–857.

Sampaolesi, M., Blot, S., D'Antona, G., Granger, N., Tonlorenzi, R., Innocenzi, A., Mognol, P., Thibaud, J.-L., Galvez, B.G., Barthélémy, I., et al. (2006). Mesoangioblast stem cells ameliorate muscle function in dystrophic dogs. Nature *444*, 574–579.

Schiaffino, S., and Reggiani, C. (2011). Fiber Types in Mammalian Skeletal Muscles. Physiol. Rev. *91*, 1447–1531.
Strober, J.B. (2006). Therapeutics in duchenne muscular dystrophy. NeuroRx J. Am. Soc. Exp. Neurother. *3*, 225–234.
Tajbakhsh, S., Rocancourt, D., and Buckingham, M. (1996). Muscle progenitor cells failing to respond to positional cues adopt non-myogenic fates in myf-5 null mice. Nature *384*, 266–270.

Théry, C., Boussac, M., Véron, P., Ricciardi-Castagnoli, P., Raposo, G., Garin, J., and Amigorena, S. (2001). Proteomic analysis of dendritic cell-derived exosomes: a secreted subcellular compartment distinct from apoptotic vesicles. J. Immunol. Baltim. Md 1950 *166*, 7309–7318.

Théry, C., Zitvogel, L., and Amigorena, S. (2002). Exosomes: composition, biogenesis and function. Nat. Rev. Immunol. *2*, 569–579.

Théry, C., Amigorena, S., Raposo, G., and Clayton, A. (2006). Isolation and characterization of exosomes from cell culture supernatants and biological fluids. Curr. Protoc. Cell Biol. *Chapter 3*, Unit 3.22.

Théry, C., Ostrowski, M., and Segura, E. (2009). Membrane vesicles as conveyors of immune responses. Nat. Rev. Immunol. *9*, 581–593.

Tidball, J.G. (2005). Inflammatory processes in muscle injury and repair. Am. J. Physiol. - Regul. Integr. Comp. Physiol. *288*, R345–R353.

Trajkovic, K., Hsu, C., Chiantia, S., Rajendran, L., Wenzel, D., Wieland, F., Schwille, P., Brügger, B., and Simons, M. (2008). Ceramide triggers budding of exosome vesicles into multivesicular endosomes. Science *319*, 1244–1247.

Uezumi, A., Fukada, S., Yamamoto, N., Takeda, S., and Tsuchida, K. (2010). Mesenchymal progenitors distinct from satellite cells contribute to ectopic fat cell formation in skeletal muscle. Nat. Cell Biol. *12*, 143–152.

Uezumi, A., Ito, T., Morikawa, D., Shimizu, N., Yoneda, T., Segawa, M., Yamaguchi, M., Ogawa, R., Matev, M.M., Miyagoe-Suzuki, Y., et al. (2011). Fibrosis and adipogenesis originate from a common mesenchymal progenitor in skeletal muscle. J. Cell Sci. *124*, 3654–3664.

Valadi, H., Ekström, K., Bossios, A., Sjöstrand, M., Lee, J.J., and Lötvall, J.O. (2007). Exosome-mediated transfer of mRNAs and microRNAs is a novel mechanism of genetic exchange between cells. Nat. Cell Biol. *9*, 654–659.

Vlassov, A.V., Magdaleno, S., Setterquist, R., and Conrad, R. (2012). Exosomes: current knowledge of their composition, biological functions, and diagnostic and therapeutic potentials. Biochim. Biophys. Acta *1820*, 940–948.

Wang, X.H. (2013). MicroRNA in myogenesis and muscle atrophy. Curr. Opin. Clin. Nutr. Metab. Care *16*, 258–266.
Wang, Y.X., and Rudnicki, M.A. (2011). Satellite cells, the engines of muscle repair. Nat. Rev. Mol. Cell Biol. *13*, 127–133.

Wang, L., Zhou, L., Jiang, P., Lu, L., Chen, X., Lan, H., Guttridge, D.C., Sun, H., and Wang, H. (2012). Loss of miR-29 in myoblasts contributes to dystrophic muscle pathogenesis. Mol. Ther. J. Am. Soc. Gene Ther. *20*, 1222–1233.

Whalen, R.G., Harris, J.B., Butler-Browne, G.S., and Sesodia, S. (1990). Expression of myosin isoforms during notexin-induced regeneration of rat soleus muscles. Dev. Biol. *141*, 24–40.
Williams, A.H., Liu, N., van Rooij, E., and Olson, E.N. (2009). MicroRNA Control of Muscle Development and Disease. Curr. Opin. Cell Biol. *21*, 461–469.

Winbanks, C.E., Wang, B., Beyer, C., Koh, P., White, L., Kantharidis, P., and Gregorevic, P. (2011). TGF-beta regulates miR-206 and miR-29 to control myogenic differentiation through regulation of HDAC4. J. Biol. Chem. *286*, 13805–13814.

Wong, C.F., and Tellam, R.L. (2008). MicroRNA-26a targets the histone methyltransferase Enhancer of Zeste homolog 2 during myogenesis. J. Biol. Chem. *283*, 9836–9843.

Yusuf, F., and Brand-Saberi, B. (2012). Myogenesis and muscle regeneration. Histochem. Cell Biol. *138*, 187–199.

Zammit, P., and Beauchamp, J. (2001). The skeletal muscle satellite cell: stem cell or son of stem cell? Differ. Res. Biol. Divers. *68*, 193–204.

Zammit, P.S., Golding, J.P., Nagata, Y., Hudon, V., Partridge, T.A., and Beauchamp, J.R. (2004). Muscle satellite cells adopt divergent fates. J. Cell Biol. *166*, 347–357.

Zatz, M., Rapaport, D., Vainzof, M., Passos-Bueno, M.R., Bortolini, E.R., Pavanello, R. de C., and Peres, C.A. (1991). Serum creatine-kinase (CK) and pyruvate-kinase (PK) activities in Duchenne (DMD) as compared with Becker (BMD) muscular dystrophy. J. Neurol. Sci. *102*, 190–196.

Zhang, C.L., McKinsey, T.A., and Olson, E.N. (2002). Association of class II histone deacetylases with heterochromatin protein 1: potential role for histone methylation in control of muscle differentiation. Mol. Cell. Biol. *22*, 7302–7312.

8. List of Publications

Saccone V, Consalvi S, Giordani L, Mozzetta C, Barozzi I, **Sandoná M,** Ryan T, Rojas-Muñoz A, Madaro L, Fasanaro P, Borsellino G, De Bardi M, Frigè G,Termanini A, Sun X, Rossant J, Bruneau BG, Mercola M, Minucci S, Puri PL. "HDAC-regulated myomiRs control BAF60 variant exchange and direct the functional phenotype of fibro-adipogenic progenitors in dystrophic muscles." Genes Dev. 2014 Apr 15;28(8):841-57. doi: 10.1101/gad.234468.113. Epub 2014 Mar 28.

L Giordani*, **M Sandoná***, A Rotini, PL Puri, S Consalvi & V Saccone (2014) Muscle-specific microRNAs as biomarkers of Duchenne Muscular Dystrophy progression and response to therapies, Rare Diseases, 2:1, e974969, DOI: 10.4161/21675511.2014.974969

Silvia Consalvi, **Martina Sandoná**, Valentina Saccone "Epigenetic reprogramming of muscle progenitors: inspiration for clinical therapies." Stem Cells Int. 2016; 2016: 6093601. Published online 2015 Dec 29. doi: 10.1155/2016/6093601

Sandonà M., Consalvi S., Tucciarone L., Puri PL., Saccone V. "HDAC inhibitors for muscular dystrophies: progress and prospects." Expert Opinion on Orphan Drugs, 4:2, 125-127, DOI: 10.1517/21678707.2016.1130617.

Luca Tucciarone*, Usue Etxaniz*, **Martina Sandoná**, Silvia Consalvi, Pier Lorenzo Puri, Valentina Saccone. "Advanced methods to study the cross-talk between Fibro-adipogenic Progenitors and Muscle Stem Cells." Book chapter on Methods in Molecular Biology, 231-256, DOI 10.1007/978-1-4939-7374-3.

Martina **Sandonà***, Silvia Consalvi*, Dr. Luca Tucciarone,

Marco De Bardi, Manuel Scimeca, Daniela Angelini, Valentina Buffa, Adele D'Amico, Enrico Bertini, Antonella Bongiovanni, Pier Lorenzo Puri and Valentina Saccone. HDAC inhibitors Modulate microRNA Content of Fibroadipogenic Progenitor-derived Exosomes to Promote Regeneration and Inhibit Fibrosis of Dystrophic Muscles. *In submission on Cell Stem Cell.*